Geochemistry Geophysics Geosystems G3

Article
Volume 11
29 October 2010
Q0AD03, doi:10.1029/2010GC003177
ISSN: 1525-2027

Published by AGU and the Geochemical Society

Pore fluid chemistry of the North Anatolian Fault Zone in the Sea of Marmara: A diversity of sources and processes

M. D. Tryon
Scripps Institution of Oceanography, University of California, San Diego, La Jolla, California 92093-0244, USA (mtryon@ucsd.edu)

P. Henry
CEREGE, Chaire de Géodynamique, Collège de France, Europôle de l'Arbois, BP80, F-13545 Aix-en-Provence CEDEX 04, France

M. N. Çağatay
Faculty of Mines, Geology Department, Istanbul Technical University, Maslak, 34469 Istanbul, Turkey

T. A. C. Zitter
CEREGE, Chaire de Géodynamique, Collège de France, Europôle de l'Arbois, BP80, F-13545 Aix-en-Provence CEDEX 04, France

L. Géli
Marine Geosciences Department, Ifremer, F-29280 Plouzané, France

L. Gasperini
ISMAR, CNR, Via Gobetti 101, I-40129 Bologna, Italy

P. Burnard and S. Bourlange
CRPG, 15 Rue Notre Dame des Pauvres, F-54501 Vandoeuvre Les Nancy, France

C. Grall
CEREGE, Chaire de Géodynamique, Collège de France, Europôle de l'Arbois, BP80, F-13545 Aix-en-Provence CEDEX 04, France

Marine Geosciences Department, Ifremer, F-29280 Plouzané, France

[1] As part of the 2007 Marnaut cruise in the Sea of Marmara, an investigation of the pore fluid chemistry of sites along the Main Marmara Fault zone was conducted. The goal was to define the spatial relationship between active faults and fluid outlets and to determine the sources and evolution of the fluids. Sites included basin bounding transtensional faults and strike-slip faults cutting through the topographic highs. The basin pore fluids are dominated by simple mixing of bottom water with a brackish, low-density Pleistocene Lake Marmara end-member that is advecting buoyantly and/or diffusing from a relatively shallow depth. This mix is overprinted by shallow redox reactions and carbonate precipitation. The ridge sites are more complex with evidence for deep-sourced fluids including thermogenic gas and evidence for both silicate and carbonate diagenetic processes. One site on the Western High displayed two mound structures that appear to be chemoherms atop a deep-seated fluid conduit. The fluids being expelled are brines of up to twice seawater salinity with an exotic fluid chemistry extremely high in Li, Sr, and Ba. Oil globules were observed both at the surface and in cores, and type II gas hydrates of thermogenic origin were recovered. Hydrate formation near the seafloor contributes to increase brine concentration but cannot explain

their chemical composition, which appears to be influenced by diagenetic reactions at temperatures of 75°C–150°C. Hence, a potential source for fluids at this site is the water associated with the reservoir from which the gas and oil is seeping, which has been shown to be related to the Thrace Basin hydrocarbon system. Our work shows that submerged continental transform plate boundaries can be hydrologically active and exhibit a diversity of sources and processes.

Components: 11,900 words, 8 figures.

Keywords: pore fluid; fluid seeps; marine hydrogeology; methane seeps; Sea of Marmara; North Anatolian Fault.

Index Terms: 1050 Geochemistry: Marine geochemistry (4835, 4845, 4850); 1065 Geochemistry: Major and trace element geochemistry; 1039 Geochemistry: Alteration and weathering processes (3617).

Received 14 April 2010; **Revised** 2 September 2010; **Accepted** 10 September 2010; **Published** 29 October 2010.

Tryon, M. D., P. Henry, M. N. Çağatay, T. A. C. Zitter, L. Géli, L. Gasperini, P. Burnard, S. Bourlange, and C. Grall (2010), Pore fluid chemistry of the North Anatolian Fault Zone in the Sea of Marmara: A diversity of sources and processes, *Geochem. Geophys. Geosyst.*, *11*, Q0AD03, doi:10.1029/2010GC003177.

Theme: Mechanics, Deformation, and Hydrologic Processes at Subduction Complexes, With Emphasis on the Nankai Trough Seismogenic Zone Experiment (NanTroSEIZE) Drilling Transect
Guest Editors: D. Saffer, P. Henry, and H. Tobin

1. Introduction

[2] Considerable attention has been given to characterizing the relationships between fluids and plate boundary fault systems at submerged convergent margins yet comparatively little is known about the hydrogeology of submerged transform boundaries. Following the 1999 Kocaeli M7.4 earthquake along the North Anatolian Fault zone at the eastern end of the Sea of Marmara, an international scientific partnership was established to identify the active faults within the Sea of Marmara through a series of cruises beginning in 2000. Early cruises [e.g., *Halbach and the Scientific Party*, 2000] identified water column methane anomalies, a shallow sulfate reaction zone, and seafloor microbial mats at the Main Marmara Fault suggesting an active hydrological system associated with the fault [e.g., *Judd and Hovland*, 2007]. The objective of the 2007 Marnaut cruise (this study) was to examine this relationship between fluid expulsion sites and active faults. The cruise occurred 12 May through 12 June 2007, aboard the French research vessel *l'Atalante* with the submersible *Nautile* with participants from France, Turkey, Italy, Spain, Germany, and the U.S. The technical objectives of the cruise were to systematically locate fluid outflow sites, via geophysical means and direct observation by submersible, to define the spatial relationship between active faults and fluid outlets, to sample these fluids to determine their nature and origin, to install instruments to monitor fluid flow, pore pressure, and microseismicity, and to sample through coring the sedimentological record of previous earthquakes. This manuscript presents and interprets the results of the pore fluid geochemical analyses.

1.1. Geologic and Tectonic Context

[3] The Sea of Marmara lies south of Istanbul, Turkey, and connects the Black Sea to the Mediterranean Sea by way of Istanbul (Bosphorus) and Çanakkale (Dardanelles) Straits. It consists of three ~1200 m deep fault-bounded extensional basins where a few kms of sediment has recently accumulated (Figure 1) separated by compressional ridges that rise ~600 m above the basin floors [*Le Pichon et al.*, 2003]. This part of the Sea of Marmara is crossed east to west by the Main Marmara Fault (MMF), which forms the northernmost branch of the North Anatolian Fault (NAF) and takes up most of the 23–27 mm/yr strike-slip motion between Eurasian and Anatolian plates [*Le Pichon et al.*, 2003; *Meade et al.*, 2002; *Reilinger et al.*, 2006]. The MMF joins the İzmit Fault in the east and the Ganos Fault in the west. The actual slip rate on the offshore MMF has mostly been estimated from models. Estimations for the dextral strike slip component vary between 12 and 23 mm/yr depending on the fault segment considered and the assumptions underlying each model [*Flerit et al.*,

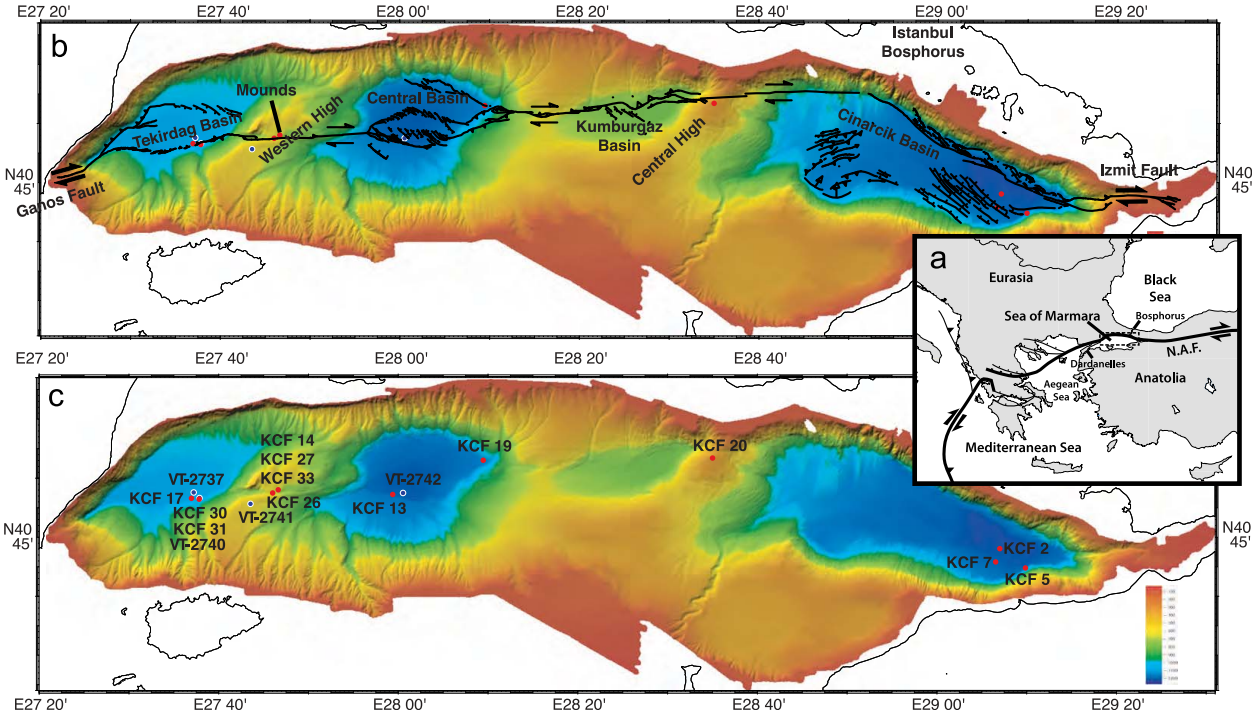

Figure 1. Map of the Sea of Marmara indicating (a) regional reference frame and tectonic framework; (b) the names and locations of major features, fault locations, and bathymetry; and (c) the locations of the coring sites referenced in this manuscript.

2003; *Hergert and Heidbach*, 2010; *Le Pichon et al.*, 2003]. Slip on secondary fault branches is less (1–5 mm/yr), but this should not bias their hydrogeological significance. The seafloor trace of the MMF is linear on the ridges, and more complex in the basins. Each sector displays different structural characteristics and tectonic styles corresponding to transtension, partitioned strike-slip and extension, or, locally, transpression [*Armijo et al.*, 2002; *Bécel et al.*, 2010; *Carton et al.*, 2007; *Rangin et al.*, 2004]. M7+ earthquakes appear to occur in the region on a ~100 yr average time interval and, after the Kocaeli M7.4 earthquake [*Barka et al.*, 2002] along the İzmit Fault, the MMF was proposed to be the likely source of a major earthquake (>M7) in the near future [*Hubert-Ferrari et al.*, 2000; *Parsons et al.*, 2000].

[4] The Sea of Marmara was a freshwater lake isolated from both the Mediterranean and Black Seas prior to the last glacioeustatic sea level rise [*Aksu et al.*, 1999; *Çağatay et al.*, 2000; *Ryan et al.*, 2003] with the transition to a marine environment occurring progressively from 14.7 to 12.4 kyr BP and with a lithological transition in sediment cores occurring at about 12 kyr BP [*Çağatay et al.*, 2000; *Vidal et al.*, 2010]. Sedimentation rates as high as 2.5 mm/yr in the basins has deposited up to 35 m of marine sediment above the lacustrine-marine transition with shelves and ridges receiving only 0.1–0.5 mm/yr [*Armijo et al.*, 2005; *Çağatay et al.*, 2000; *Mercier de Lépinay et al.*, 2003]. Presently, the water of the Sea of Marmara is strongly stratified with a 20–40 m thick layer of brackish Black Sea-water entering through the Bosphorus capping warm saline Mediterranean water that enters through the Dardanelles and sinks below the cap.

1.2. Prior Evidence for Fluid Emissions

[5] Methane emissions associated with the Main Marmara Fault were found during the Meteor cruise M 44/1 (1999), as evidenced by black-grayish seafloor sediments with bacterial mats and by methane anomalies in the lower part of the water column [*Halbach and the Scientific Party*, 2000]. These observations were made where the fault crosscuts the Western High separating the Tekirdağ and the Central basins. In addition, a shallow sulfate-methane reaction zone (SMRZ) was detected in sediment cores from the same area at depths of 4 to 5 m below the seafloor and from the Çınarck Basin at 3 mbsf [*Çağatay et al.*, 2004]. High-resolution seismics [*Le Pichon et al.*, 2001] and chirp profiles indicated the probable presence of trapped gases within the uppermost sedimentary sequences.

Observations during the Marmarascarps cruise (2002) showed that bubbles (presumably of methane) are often present immediately beneath the seafloor at reduced sediment patches, notably on the Western High. More spectacular active chimneys were found in Tekirdağ Basin and in the Central Basin [*Armijo et al.*, 2005] but the fluids were not sampled. In Tekirdağ Basin, fluid outflow is visible, due to a contrast in optical indices; however, the temperature is less than 0.5°C above the bottom water temperature, implying that a fluid of very different salinity is expelled at this site. Water sampled below the SMRZ in cores taken in these basins and on the Western High exhibited decreasing salinity with depth. *Zitter et al.* [2008] suggested that the burial of Lake Marmara fresh or brackish water was the source of the freshened end-member fluid seen at deep levels in cores from the Marmara-VT cruise and at the chimneys. Reasoning based on the extrapolation of mixing lines suggested a minimum chlorinity of 100 mM for the buried fluid, thought to be representative of the Marmara glacial lake. These Tekirdağ chimneys were found on the MMF outcrop and are located on a recent seafloor rupture (possibly of 1912 Ganos earthquake), which broke older carbonate crusts. In the Central Basin, smaller chimneys and abundant carbonates were found on the subsidiary fault bounding the basin to the north. This fault does not display evidence of comparable recent surface rupture. Manifestations of fluid expulsion in the Çınarck Basin area were not systematically investigated previously but intense expulsion of methane in the İzmit Gulf near the 1999 Kocaeli earthquake rupture have been reported [*Alpar*, 1999].

1.3. Spatial Relationship Between Fluid Flow and the MMF

[6] The Sea of Marmara is an exceptional case were active seafloor venting sites are found on the surface trace of a major plate boundary fault. The distribution of seeps in convergent margins is often more complex with rare, if any, seeps at the frontal thrust and the bulk of fluid outflow distributed over the outer fore arc at the surface traces of thrust faults, normal faults, and mud volcanoes. Our observations in the Sea of Marmara suggest a simple pattern where the main strike-slip fault is the main channel for fluid expulsion on the ridges and the basin bounding faults are the main fluid channels in the basins. This simple pattern is overlain by the effects of turbidite channels which provide lateral conduits, local structural effects such as anticlines which can act as traps, and by local bends in the MMF causing compaction or dilation driven flow. In addition, temporal influences such as recent earthquake activity may affect emissions. For example, the region of the Central High seismic gap exhibits less gas emissions while the region west of the Kocaeli earthquake rupture that exhibits microseismic activity exhibits extensive gas emissions [*Géli et al.*, 2008].

[7] The spatial relationship between fluid seeps and the faults was constrained by a combination of previously collected subbottom seismic surveys that located the fault structures[*Armijo et al.*, 2002, 2005; *Demirbag et al.*, 2003; *Imren et al.*, 2001; *Rangin et al.*, 2004] and also imaged blanking caused by gas in the sediment column [*Le Pichon et al.*, 2001; *Zitter et al.*, 2008], by water column acoustic surveying that imaged bubbles in the water column [*Géli et al.*, 2008], and by visual surveys by submersible. Indications of flow included gas expulsion, visible aqueous outflow, areas of black sulfidic sediment, and characteristic seep biology such as microbial mats and chemosynthetic bivalves (see reviews by *Judd and Hovland* [2007] and *Levin* [2005]). In the basins, fluid seeps were restricted to a few 10s of meters of the bounding faults which were well located by fault scarps. The one significant exception to this was in the southern Çınarck Basin where more widely distributed seepage was observed associated with a broad region of closely spaced normal faults rather than a simple bounding fault. On the ridges, fluid seepage was associated with the main strike-slip fault but also extended along anticlines.

2. Methods

2.1. Sampling Strategy

[8] The acoustic method of gas plume detection described by *Géli et al.* [2008] was extremely efficient and allowed us to discover many new seep sites and to firmly establish the direct correspondence between water column acoustic anomalies, seafloor seeps, and active faults. After acoustic identification of potential seep sites we visually confirmed and explored the sites utilizing the *Nautile* submersible. Ten cold seep sites spanning the fault zone were explored during 30 dives. Sites for coring were chosen, based on a combination of prior geophysical surveys, our acoustic bubble detection results, and our visual surveys, to include a diverse and representative sampling. Thirteen piston cores of up to 10 m were collected in and near the seep areas, as well as background cores, and utilized for pore fluid

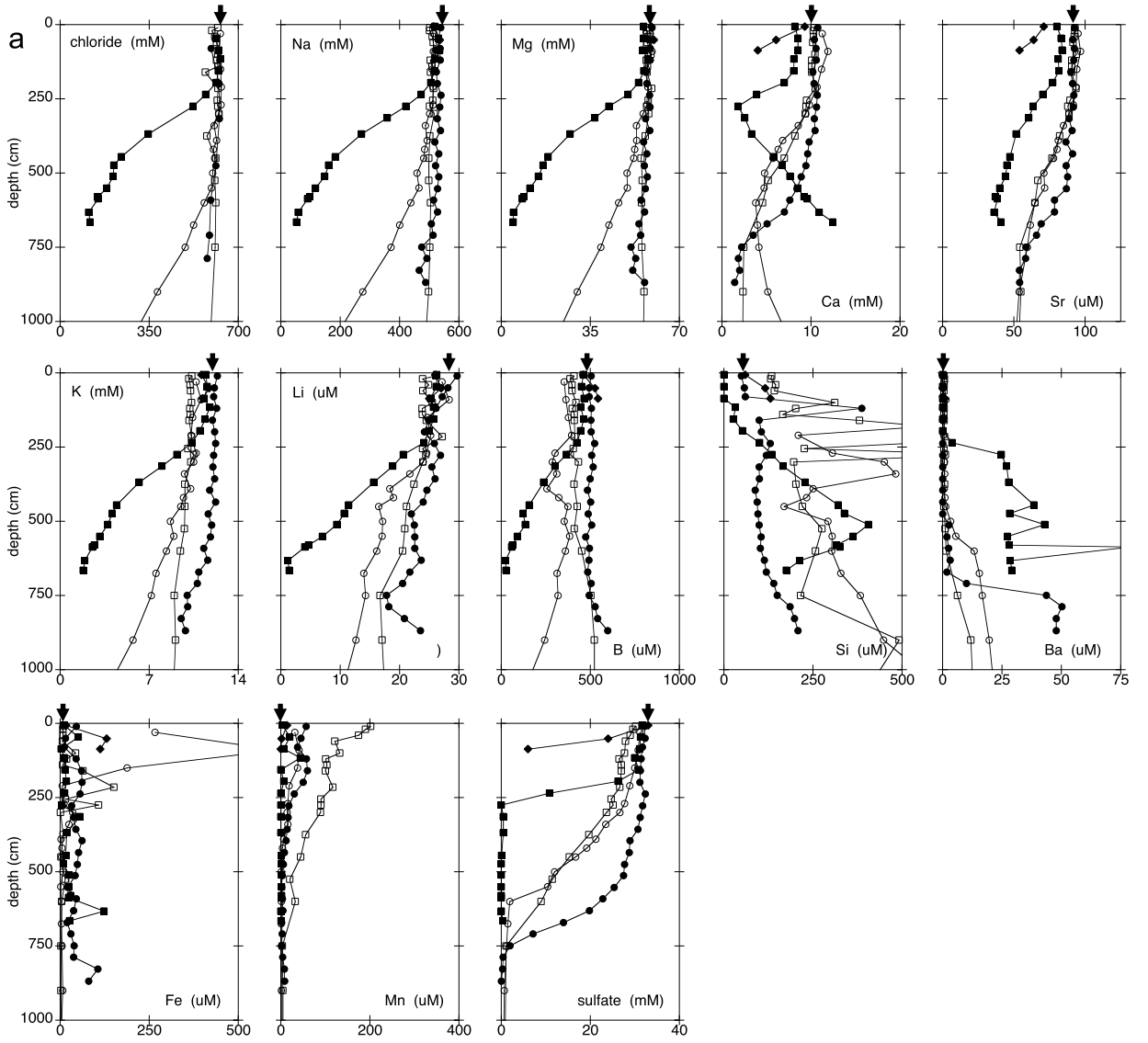

Figure 2. Results of the core pore fluid analyses. (a) Tekirdağ Basin, (b) Çınarck Basin, (c) Central Basin, (d) ridge sites, and (e) Western High mound sites. See section 3 for details.

analysis (Figure 1). Coring was carried out with the IFREMER 10 m Kullenberg piston coring system.

2.2. Analytical Methods

[9] Upon recovery, the cores were rapidly sectioned to 1 m lengths on deck, capped, and moved to the 4°C cold room. Fluid was extracted at intervals along the core by utilizing Rhizon samplers [*Dickens et al.*, 2007; *Seeberg-Elverfeldt et al.*, 2005]. Rhizon samplers are made of a 2.4 mm hydrophilic porous polymer tube with a pore size of 0.1 μm attached to PVC tube and luer connector. The polymer tube is supported by a nylon wire. The core liner is drilled at appropriate intervals and the sampler inserted until it seals against the liner. For this study we either attached the luer to a syringe needle which was then inserted into evacuated plasma vials or attached the luer to a 10 ml syringe and extracted the plunger and affixed it at full extension creating the needed vacuum for extraction. Typically 5 ml of fluid was extracted from the shallowest levels (0–2 m) and this was reduced downcore to as little as 1–2 ml near the bottom, depending on the core's properties. The primary reason for this sampling technique was to preserve the cores for subsequent physical property and sedimentological work. This technique also provided

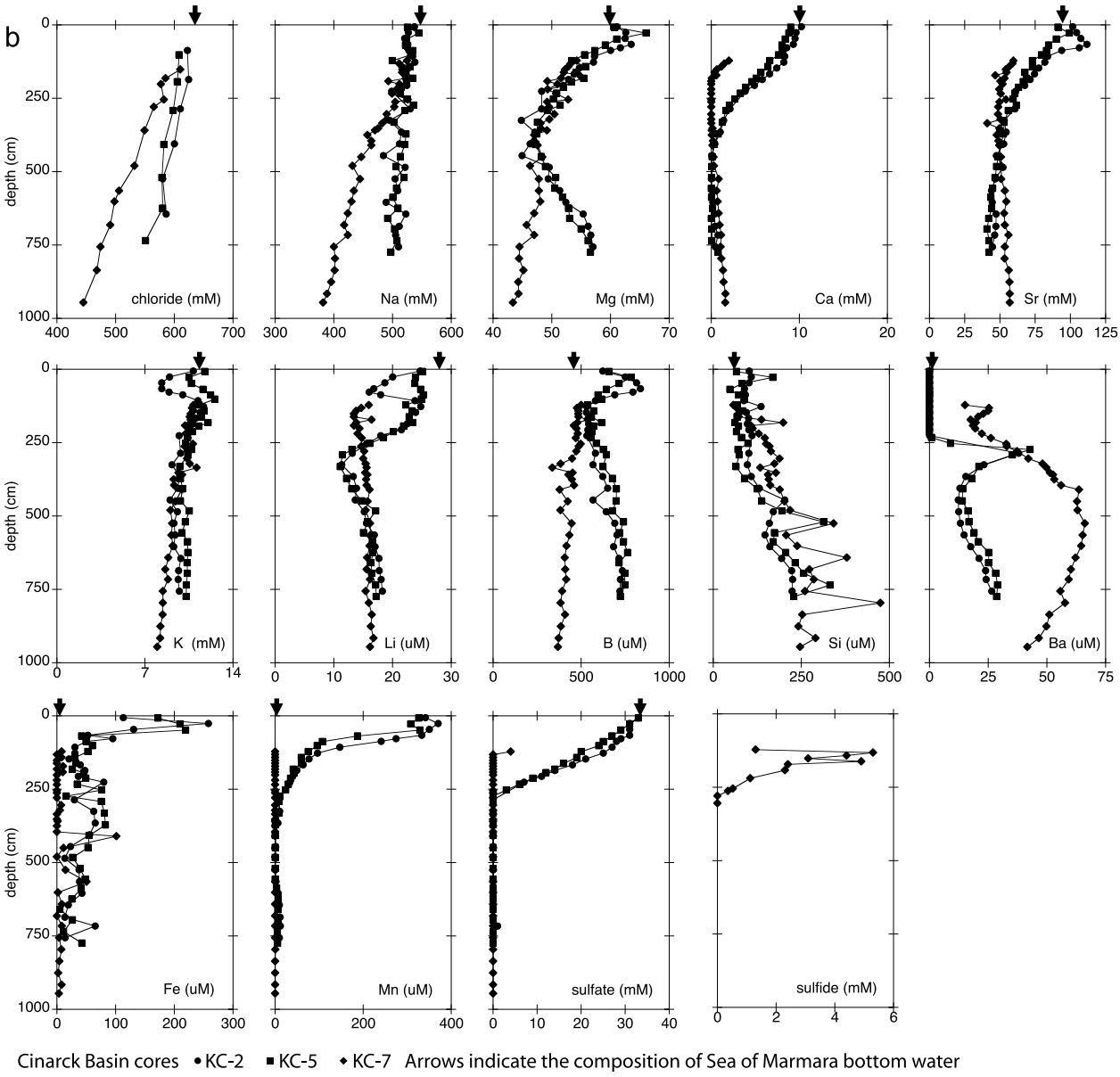

Figure 2. (continued)

excellent filtration and minimized fluid contact with oxygen.

[10] The fluids were subsampled in the cold room immediately after collection. When sufficient fluid was collected, 3 ml of sample was quickly transferred to a 4 ml vial, 0.40 ml of 0.25 M Zn acetate added, and the vial capped, shaken, and stored. This pretreatment method precipitates the sulfide allowing for storage for onshore analysis many weeks later by standard colorimetric methods. For all fluids collected, 1 ml subsamples for elemental analysis were acidified to prevent precipitation and preserve them for onshore analysis. The remaining fluid was saved for other analyses and archiving. Chloride concentration was determined on board from these latter samples by titration with silver nitrate with the indicator potassium chromate/potassium dichromate using IAPSO seawater as the standard. Onshore elemental analyses were done via ICP-OES. Sulfide and ammonia were analyzed by standard methods [*Gieskes et al.*, 1991].

[11] Cores were scanned on a GEOTEK multisensor core logger (MSCL) and these logs used to quantify voids in the cores and correct the sampled

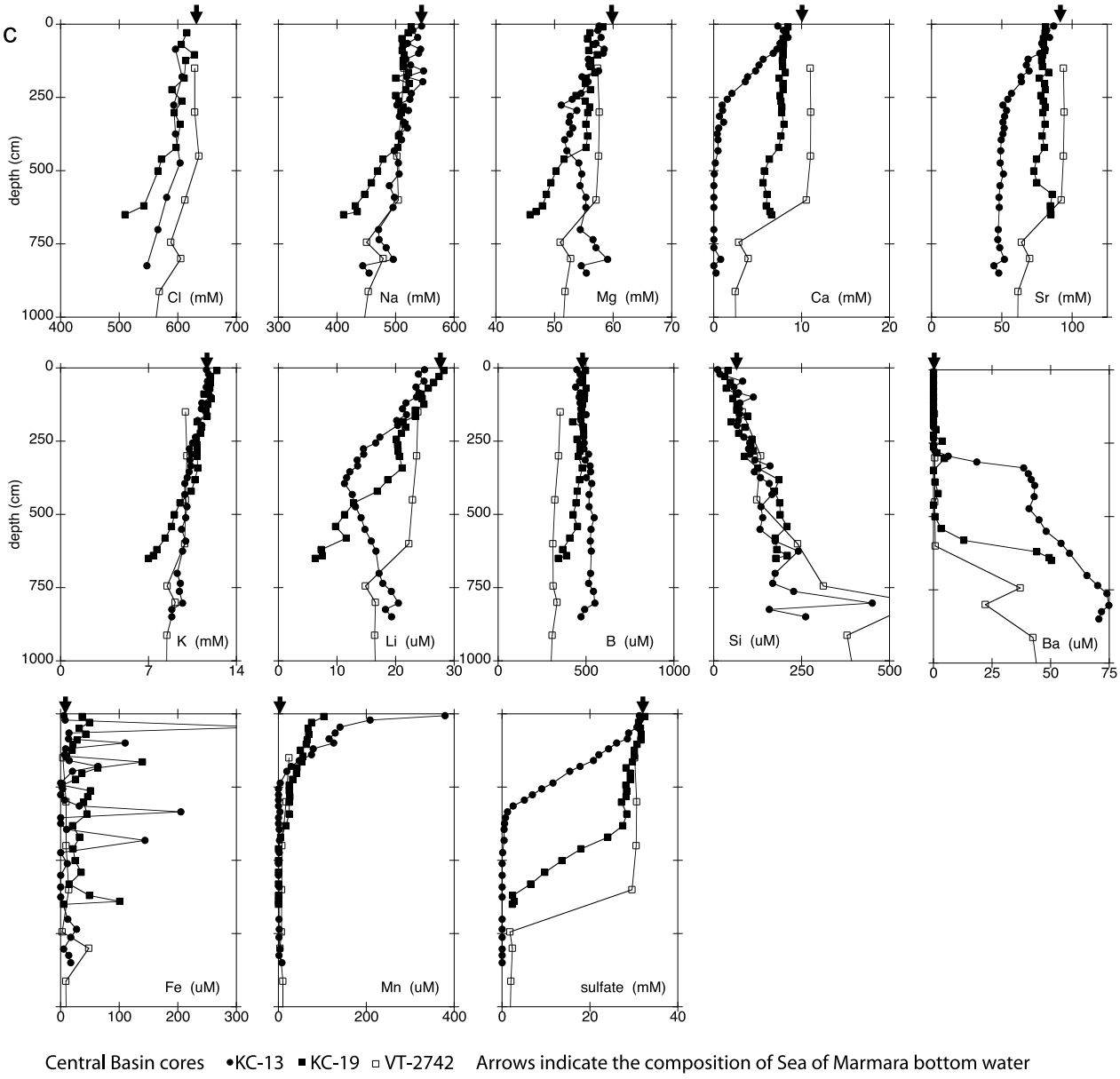

Figure 2. (continued)

depth intervals for expansion. The MSCL profiles were also used for correlation of the interface and piston cores recovered from the same location, which is important for checking if the piston core tops were missing. All depths reported here are corrected rather than indicated depth.

3. Results and Interpretations

[12] The tectonic environments of the seeps varied from basin bounding extensional faults to strike-slip faults, many of which exhibited sharp and fresh-appearing fault escarpments. Most seeps were extensive, patchy, and diffuse, displaying patches of black sulfidic sediment with typically white to yellow/orange microbial mat on the surface. One end-member type was highly focused, emitting ambient temperature shimmering fluids of low salinity that precipitated chimney structures. At other sites gas bubbles were seen coming from the sediment and, in one occurrence, from open fractures in underlying sedimentary rocks. Another type had the appearance of a flow with precipitate covered sediment with a fan morphology extending downslope from the seep. This latter site was associated with very high salinity fluids and significant

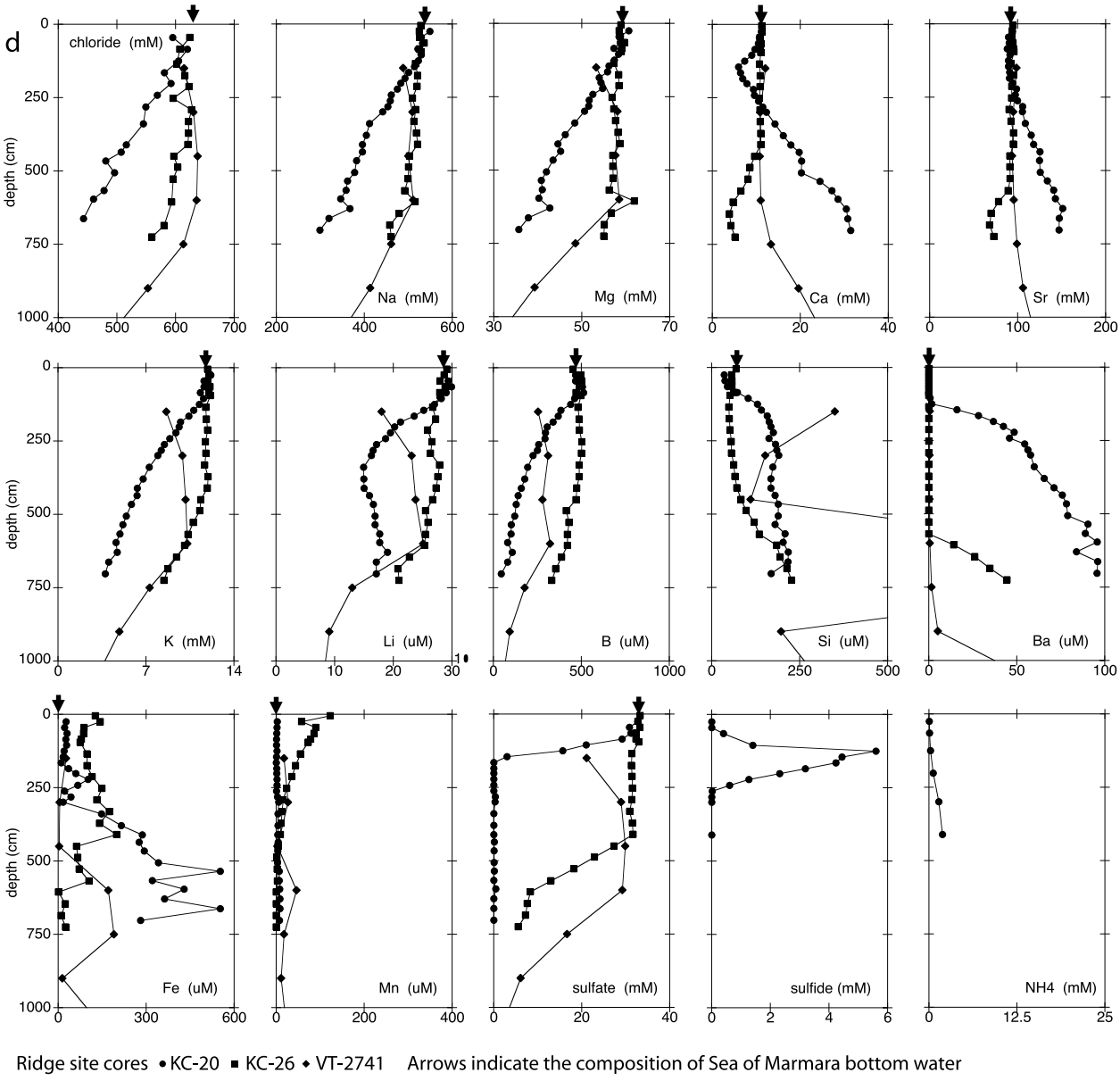

Figure 2. (continued)

traces of hydrocarbons and included shallow gas hydrate well outside the methane hydrate stability field.

[13] The concentration profiles of Cl^-, Na^+, Mg^{2+}, Ca^{2+}, Sr^{2+}, K^+, Li^+, B, Si, Ba^{2+}, Fe, Mn, sulfate, sulfide, and NH_4 are shown in Figure 2. They are grouped by location: Tekirdağ Basin, Çınarck Basin, Central Basin, Ridge sites excluding the two hydrate and carbonate mounds, and the hydrate and carbonate mounds. This grouping facilitates discussion and appropriate scaling of the axes for the wide ranges of concentrations encountered. Core locations are shown in Figure 1. Average bottom water composition is indicated in Figures 2a–2e by arrows.

3.1. Basin Sites

[14] Figures 2a–2c show the downcore chemical profiles of the Marnaut basin cores with Marmara-VT cores VT-2737, VT-2740, and VT-2742 included for reference [*Zitter et al.*, 2008]. Cores KC-2 and KC-13 were taken as reference at sites without nearby seafloor manifestations of gas or water outflow. Cores KC-17, VT-2737 and VT-2742 are

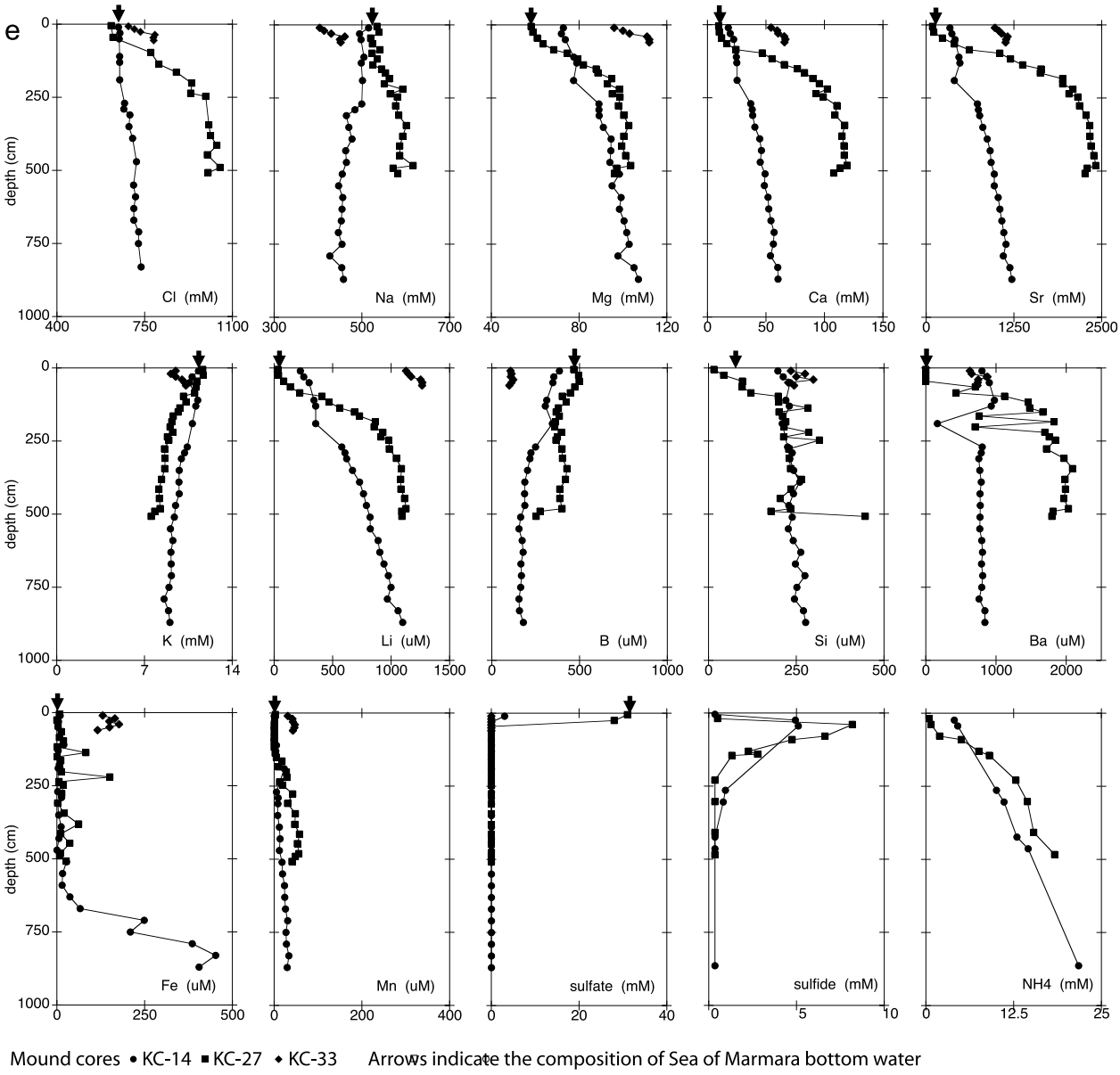

Figure 2. (continued)

located about 1 km from known cold seep sites but with chirp profiles indicating the presence of free gas in the sediment. The fluid compositions of these and the background cores are dominated by shallow redox reactions and carbonate precipitation. A freshening gradient with depth is also observed to various degrees in Cl and Na profiles. KC-2, KC-5, and KC-13 exhibit a shallow sulfate-methane reaction zone (SMRZ) extending down to the sulfate-methane interface (SMI) at about 300 cm depth. The shallow SMI and linear SMRZ are typical of anaerobic methane oxidation (AMO) [*Borowski et al.*, 1996, 1997]. AMO produces bicarbonate which reacts with seawater Ca, Mg, and, Sr to produce carbonates, leading to the observed minima of these ions coinciding with the SMI. KC-17 and the VT cores exhibit a similar pattern, but with a deeper SMI at 750 cm depth. Below the SMI in all cores Ba concentrations increase due to dissolution of biobarite in the absence of sulfate ions. Cores KC-7, KC-19, KC-30, KC-31 and VT-2740 were collected near and at fluid seeps and are altered with respect to the basin background profiles and notably display stronger freshening gradients with depth,

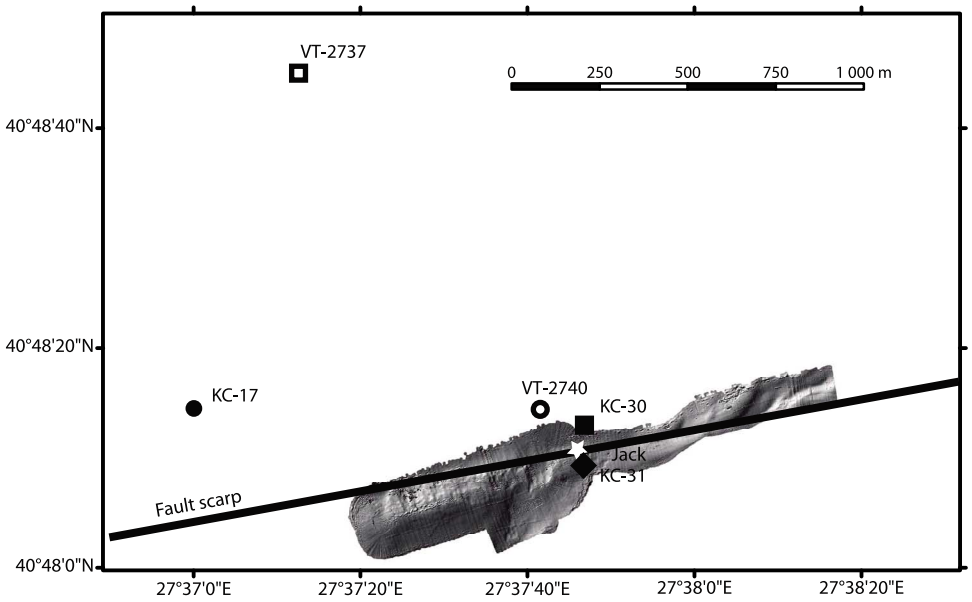

Figure 3. Detail map of structure and site location at the Tekirdağ Basin site.

indicative of upward advection of low-salinity pore fluid.

3.1.1. Tekirdağ Basin

[15] All of the Tekirdağ Basin (Figure 2a) cores were taken at the southern margin at a depth of 1120 m near the site referred to as "Jack the Smoker" [*Armijo et al.*, 2005]. Figure 3 shows the spatial relationship between the cores. Locations are estimated to be ±25 m. Marmara-VT cores 2737 and 2740 are also shown in Figure 3 and in the pore fluid composition plots for reference [*Zitter et al.*, 2008]. KC-31 was taken above the fault scarp at the Jack the Smoker site in Tekirdağ Basin and only one meter was recovered which appears to be the core top. These cores are dominated by the influence of Lake Marmara brackish water. In particular, core KC-30, taken adjacent to the site "Jack the Smoker," exhibits strong freshening with depth. Crossplots of the relatively unreactive pore fluid chemical components against chloride can be used to estimate the composition of the end-member fluid (Figure 4). This is in close agreement to the estimate made by *Zitter et al.* [2008] and used in their diffusion profile model 2. There is evidence, however, that these fluids have been involved in silicate diagenesis. The Na/Cl molar ratio of 0.5 of the end-member fluid is significantly less than typical lake, river, and meteoric water, as well as seawater and presumably this is due to Na uptake during clay formation from silicates such as feldspars which would also take up K and Mg and release Ca. There is a very clear progression of composition profiles with distance from the fluid vent site. KC-17 and VT-2737 are located ~1500 m from the vent and have chloride profiles similar to one another. KC-17 is much closer to the fault scarp, however, which might suggest that the vent is a point source with minor lateral leakage along the fault, or that there is simply a maximum distance from the fault beyond which flow along it has minimal influence. Alternatively, KC-17's nearly vertical profiles of Ca, Sr, and sulfate in the top ~500 cm followed by a concave upward lower section suggest that there may be downward flow at this site while VT-2737 appears more linear and diffusive.

3.1.2. Çınarck Basin

[16] Core KC-2 was taken at a depth of 1280 m in the east central Çınarck Basin (Figure 2b) and was intended as a representative background core. KC-5 was located at the base of the southern scarp in a small fault-bounded and sediment-filled depression at a depth of 1270 m. The pore fluid profiles from these two cores are nearly identical and distinguish themselves from the other basin cores by their unusually high boron content. This is not surprising considering that more than 60% of the world's boron reserves are located in Turkey and much of that is located in the 30,000 km^2 Susurluk Drainage Basin, south of the Sea of Marmara, which drains into the Çınarck Basin [*Kazancı et al.*, 2006]. These cores also exhibit a shallower sulfate-methane reaction zone depth than most basin cores. The small decrease

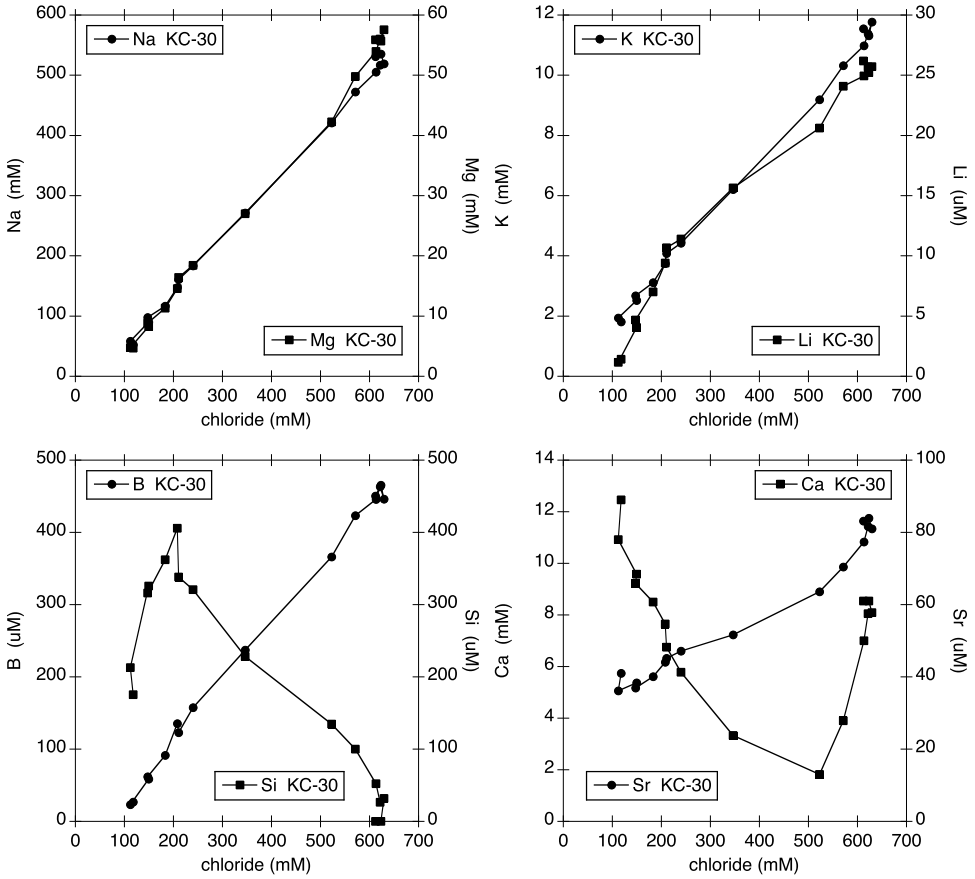

Figure 4. Crossplots of major ions versus chloride for the core KC-30 showing graphically the determination of the Pleistocene Lake Marmara end-member composition. Generally, the lowest concentration Cl sample is also the lowest concentration of the other ions; however, as can be seen in the plots, shallow diagenetic processes have a large affect on Ca and Si, and therefore, Lake Marmara bottom water concentration of these ions cannot be readily determined but are presumed to also be that of the lowest Cl concentration.

in sulfate in the first 100 cm followed by a rapid and linear decrease to zero at 300 cm, combined with the sharp decrease in Mn at 100 cm or shallower, suggests that the anoxic boundary occurs by 100 cm depth in these cores. The unusually steep sulfate gradient and shallow SMI are indicative of upward methane flux and consumption of sulfate by AMO.

[17] Sharp changes in Mg, Li, K, and B above 400 cm suggest silicate diagenetic processes may also be occurring in addition to the typical redox and carbonate reactions. Silicate mineral weathering such as kaolinite formation from feldspar are typically sinks for these elements. The increase in Mg below this may relate to Mg aragonite to calcite reprecipitation.

[18] Core KC-7 was obtained at 1215 m water depth southwest of the other two in an area of widespread extensional faulting and in an extensive but heterogeneous patch of bubble emissions, black sulfidic sediment, small carbonate concretions, and microbial mats. Comparison of the MSCL profiles of KC-7 and Interface core KI-07 obtained from the same location showed that approximately the top 1–1.3 m of KC-7 was missing. Further, the shallowest samples (10 cm intervals for the first 100 cm) are far removed from bottom water values for many components and, when combined with the extensive gas expansion voids observed in the core (a cumulative 1.3 m), corroborates that the core top was lost on recovery. The pore fluid composition is distinct from KC-2 and KC-5 primarily in that the SMI is closer to the sediment surface (even after correction for core loss) and it exhibits a much greater level of freshening with depth reaching 70% of bottom water value at 950 cm. Ca, Mg, and Sr are consumed in the SMRZ which is presumably 1 to 1.5 m thick at this site. Less reactive components such as K and Na fall on a mixing line between bottom water and the brackish end-member proposed earlier. The

steepening of the Cl, Na, and K gradient, compared to KC-2 and 5, suggests a greater aqueous flux, yet insufficient to impart curvature to the profile over the range of the core depth as seen at core KC-30 from the Tekirdağ site.

3.1.3. Central Basin

[19] Core KC-13 and VT-2742 were collected within the Central Basin (Figure 2c) at a water depth of 1250 m near the southern inner bounding fault scarp. Gas blanking was evident in subbottom profiles at site VT-2742 and seeps observed at the fault scarp [*Zitter et al.*, 2008], but neither was observed at site KC-13 located east along the same fault. KC-13 exhibits chemical profiles that are nearly indistinguishable from KC-2 and KC-5 in the Çınarck Basin with minor exceptions: a vertical B profile at seawater values, a ~50 cm deeper SMI with a less pronounced Mg minimum at the SMI, and significantly higher Ba concentrations below the SMI. KC-19 was taken at the eastern end of the Central Basin at a depth of 1170 m where one active fault branch connected to the MMF on the central high reaches the edge of the basin. Small precipitation structures, visible venting, and extensive biological activity were seen here during the Marnaut and previous cruises. Downcore freshening is similar to other cores taken at fluid emission sites but is only observed below 4 m depth. KC-19 also may show signs of deeper silicate diagenetic reactions. The concentrations of Na and K, often diagnostic of silicate weathering, fall below the mixing line between bottom water and Lake Marmara water and are thus depleted.

3.2. Ridge Sites

[20] Cores KC-14, KC-26, KC-27, and KC-33 were collected on the Western High where it is cut by the MMF and KC-20 was taken south of the MMF on the eastern section of the Central High, between the Kumburgaz and Çınarck Basins (Figures 2d and 2e). While the basin pore fluids appear to have a common source of Pleistocene Lake Marmara water that has been modified to various degrees by microbial and diagenetic processes, the chemical composition of the ridge site pore fluids suggests they are also influenced by gas hydrate formation and decomposition near the seafloor as well as deep sourced fluids possibly associated with natural gas reservoirs. Most notable in this respect is the occurrence of gas hydrate in some of the cores collected on the Western High and the observance of oil seeping from the sediment in this area. At a depth of 660 m and a temperature of 14.5°C, these hydrates are well outside the stability field of methane hydrates. Analysis of the hydrates confirmed the presence of higher hydrocarbons at concentrations that allow the formation of hydrates at the in situ P, T conditions [*Bourry et al.*, 2009]. No evidence of gas hydrates was observed at any other site in the Sea of Marmara in spite of ample evidence of gas. Presumably, this is because the gas sampled at the other sites is mostly methane, with less than 1% of other hydrocarbons, and only the deepest parts of the basins reach the upper boundary of the methane hydrate stability field [*Bourry et al.*, 2009].

[21] KC-20 was the only core recovered on the Central High and was taken in an area where acoustics indicated gas in sediments and the water column. It was located south of the trace of the MMF across the high separating the Kumburgaz and Çınarck Basins at a water depth of 335 m, the shallowest of the Marnaut cores. The core exhibits a shallow SMI of 150 cm and associated Ca minima and sulfide maxima (Figure 2d). Significant freshening occurs with depth, comparable to KC-7 in the Çınarck Basin. These two observations suggest a moderate level of advective flow. The profiles of all chemical components in this core do not fall on a mixing line between bottom water and Lake Marmara water but rather K, B, Li, Mg, and Na fall significantly below (depleted) (Figure 5) and Ca, Sr, and Ba increase with depth (Figure 2d). This is consistent with silicate mineral diagenesis.

[22] Cores KC-14, KC-26, KC-27, and KC-33 were collected on the Western High at 660 m where the MMF cuts across it from the Central Basin to the Tekirdağ Basin. KC-26 was taken in the fault valley and the other cores on two mounds located north of the fault (Figure 6). Marmara-VT core VT-2741 was taken ~3 km south of the MMF and 7 km WSW of the mounds and is included for reference. The mound site produced a large bubble plume visible on the high-frequency acoustics [*Géli et al.*, 2008] and there was also an oil slick on the surface waters visible during multiple visits. The mounds have a high sonar backscatter in a wide frequency range (at least 35–200 kHz) and chirp profiles through the mounds suggested that they were small mud volcanoes which formed along a NE–SW anticlinal ridge north of the MMF (P. Henry and the Marnaut Scientific Party, Marnaut expedition cruise report, 85 pp., 2007, available at http://www.cdf.u-3mrs.fr/~henry/marmara/marnaut_

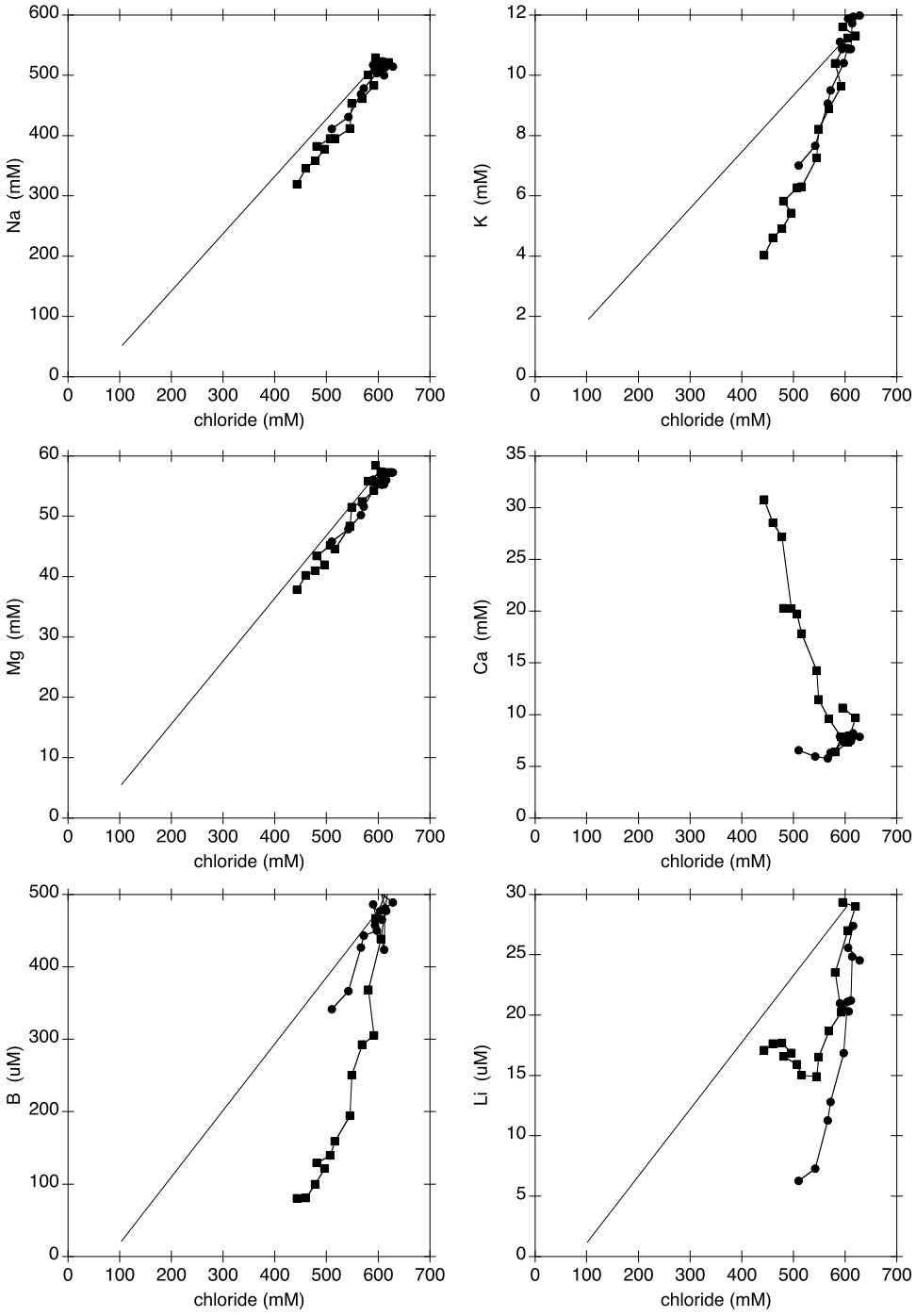

Figure 5. Chloride crossplots showing proposed effects of silicate mineral diagenesis. Lines are mixing line between Marmara bottom water and Lake Marmara water. Ions that plot below the lines are depleted and those above are increased in pore waters. This pattern is consistent with typical silicate diagenetic process.

public/marnaut_final_reports). No mud breccia was found in the cores, however, which instead appeared formed of hemipelagic sediment bearing several authigenic carbonate layers in the first 2.5 m, as well as barite. Although earlier stages may have involved mud extrusion, there is no evidence for current activity. The northern mound is circular, 150 m diameter, with a depressed center and irregular rim. The southern mound is similar in size and shape with a breach in its NE wall. This site thus appears as chemoherms formed on long-lived fluid conduits. These structures appear quite similar to the

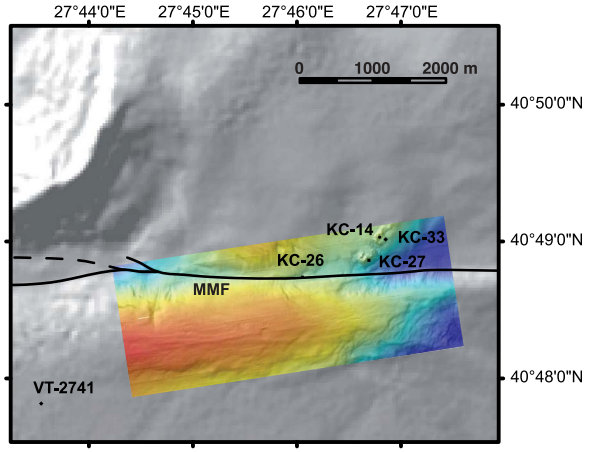

Figure 6. Detail map of the hydrate and carbonate mound site. Inset is AUV high-resolution microbathymetry from the 2009 Marmara-DM cruise. The mounds are significantly offset from the Main Marmara Fault (MMF) which is easily traced in the bathymetry. Coring site locations from Marnaut and Marmara-VT are shown.

larger fluid escape mounds observed on the Costa Rica margin [*Klaucke et al.*, 2008]. Thus, they are suspected to be partly caused by the accumulation of subsurface methane-derived authigenic carbonate and partly by subsurface accumulation of gas hydrates [e.g., *Hovland and Svensen*, 2006]. Bottom surveys with the Nautile submersible revealed extensive bubble streams and globules of oil coming from the sediment in many places. One of the main bubble fields was on the top of the northern mound, located 700 m north of the MMF trace, and core KC-14 was taken nearby. On the southeast and south slopes of the mound, two sites of fluid expulsion were seen where the flow appeared to be focused through outlets <1 m across exhibiting flow of dense water, as evident from the downslope pattern of flow channels and white barite precipitate (Figure 7). Core KC-33 was taken as close to these outlets as our navigation allowed. KC-27 was taken at the second mound, 400 m to the southwest, which appeared to be somewhat less active based on biology and bubbles. KC-27 and KC-33 contained hydrates and all but 1 m of 33 was lost to degassing. The recovered meter of KC-33 appeared to be the core top but we cannot be certain of this. Regardless, its composition is comparable to the deepest part of KC-14 and this is useful in the overall characterization of the fluids at this site. KC-27 remained intact and we successfully extracted the fluids.

[23] Core KC-26 from the fault valley has essentially the same chemical profiles of all elements as the background core VT-2741 and the non-seep basin cores KC-17, VT-2737, and VT-2742. The composition of KC-14, KC-27, and K-33 are highly altered from that seen at other sites and is likely a result of multiple sources and processes that will be discussed in section 4.

4. Discussion

4.1. Flow Rates

[24] Freshening due to mixing with buried brackish water from the Marmara Lake is observed at all sites except at one location of the Western High were fluids having a salinity higher than seawater are expelled. Even at locations with no fluid flow through the seafloor, the change in water salinity after the reconnection with the Mediterranean Sea 14.7 kyrs BP [*Vidal et al.*, 2010] is expected to cause a freshening gradient within the sediment. For a chloride diffusion coefficient in the sediment of 10^{-9} m^2/s, the chlorinity gradient at the seafloor in a pure diffusion model is 13.5 mM/m [*Zitter et al.*, 2008]. Taking into account uncertainties in diffusion coefficients, on the timing of the salinization, on true depth, and on the salinity of the end-member fluid, any gradient deviating by more than ±5 mM/m from this value in the first 10 m below the seafloor almost certainly indicates fluid movement with respect to the seafloor. Furthermore, profile curvature at the 10 m scale indicates vigorous advection at rates in the mm/yr range or more. It follows that coring sites can be classified between sites with no net water outflow or downflow (KC-2, KC-5, KC-13, KC-17, KC-26, VT-2737, VT-2741, VT-2742), sites with local outflow on the order a mm/yr (KC-7, KC-19, KC-20, KC-26, KC-31, VT-2740) where the gradient of chlorinity is increased, and one site where upward fluid velocity can be estimated from the shape of the profile (KC-30). Fluid velocity is determined to be 10 to 15 mm/yr for this core by fitting data below 2 m depth with a steady state advection-diffusion model [e.g., *Martin et al.*, 1996]. Fluids expelled though the carbonate mound have higher chlorinity than seawater. In core KC-27, the curvature of the chlorinity profile above the depth at which gas hydrates were sampled indicates upward fluid flow at a velocity of about 20 mm/yr. In core KC-14, advection rate is too low to cause significant curvature, and no hydrate was found. Subsurface fluid flow is a complex process and flow rates are both spatially and temporally heterogeneous [e.g., *Tryon et al.*, 2002] so these rates should not be extrapolated to the scale of the mounds but may be indicative of

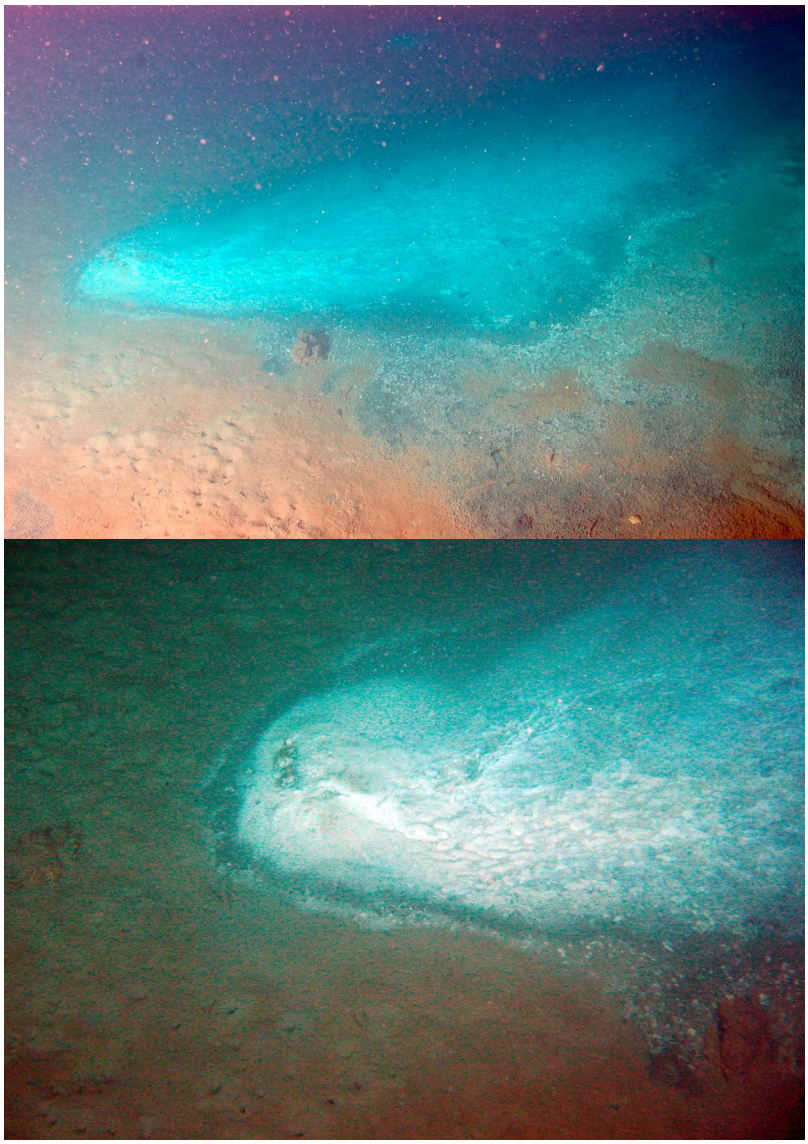

Figure 7. Seep site near KC-33 showing downslope flow pattern of dense fluids (down is to the right in the photo). White material is barite precipitate, black ring is sulfidic sediment, and white halo outside that is microbial mat.

the order of magnitude of flow in these locations. Overall, these results are comparable with typical rates in areas of faulting in marine sedimentary environments such as convergent and passive margins [e.g., *Luff et al.*, 2004; *Torres et al.*, 2002; *Tryon et al.*, 2002; *Tryon and Brown*, 2004].

4.2. Fluid Sources

[25] Sources of pore fluids in the Sea of Marmara are significantly different than in typical ocean basin or margin environments. The continental setting replaces igneous oceanic basement with primarily metamorphic rocks of sedimentary origin and its recent period as a lacustrine environment adds fresh water to the sources. The mix of bottom water, Lake Marmara brackish water, and deep sources associated with the fault zone and/or gas reservoirs can be overprinted with silicate and carbonate diagenetic processes and, at the mound site, removal of water during gas hydrate formation. These multiple sources and processes cause the genesis of some of these fluids and their initial compositions to be not readily determined. Some general observations and interpretations can, however, be made which can bracket the sources and processes involved.

[26] Major ion concentrations at most sites in the Sea of Marmara can be modeled from the mixing of two components. The basin core pore fluids are dominated by simple mixing of a present-day bottom water upper end-member with a brackish, low-density Lake Marmara end-member that is advecting buoyantly and/or diffusing from a relatively shallow depth. This mix is overprinted by shallow redox reactions and carbonate precipitation that consumes methane, sulfate, Ca, Mg, and Sr, and produces carbonates and sulfides. Some traces of low-temperature silicate diagenesis are also present as well as traces of thermogenic gas but, in general, no deep source fluid is apparent in the basin and basin margin cores.

[27] The most altered fluids sampled at core KC-20 on the Central High are compatible with mixing of 60% seawater and 40% brackish water with an overprinting of local low-temperature silicate diagenesis. The profiles of K, B, Li, Mg, and Na fall significantly below the mixing line between seawater and Lake Marmara water, consistent with low-temperature silicate mineral diagenesis (Figure 5). Ca-bearing silicate minerals such as plagioclase feldspar are common components of basin sediment in continental environments and these weather to form a variety of authigenic clay minerals such as kaolinite. A large number of different weathering reactions are possible depending on the abundance of different silicate minerals and available cations but all ultimately consume cations such as K, B, Li, Mg, and Na and release Ca [e.g., *Gieskes and Lawrence*, 1981; *Martin et al.*, 1996]. Ca, Sr, and Ba increase with depth (Figure 2d). Ba and Sr are common elements in sedimentary rocks and would be expected to be released. The weathering of K feldspar and mica contribute Ba and Sr to pore fluids and the dissolution of biobarite and recrystallization of calcite below the SMI may also be involved in the increase in these elements. Gas collected on dive 1664 near this site was analyzed and found to be primarily methane with a thermogenic origin [*Bourry et al.*, 2009] suggesting the possibility that there may be an additional deep source of fluids. Silicate diagenetic processes at this source or as a result of fluid-rock interaction during gouge formation in the MMF zone may contribute to the observed composition.

[28] The three mound cores exhibit the most overwhelming evidence for deep-sourced fluids and deep processes including, most notably, thermogenic gas and oil. One method for estimating the source temperature and depth is the use of geothermometers. In a recent review of available geothermometers, those based on Na-K and silica appeared as the most reliable, at least for crustal hydrothermal systems [*Verma et al.*, 2008]. Li-Mg and Li-Na geothermometers have been proposed for sedimentary basin fluids, notably these associated with oil [*Kharaka and Mariner*, 1989]. Application of these geothermometers to fluid expelled through deep-sea mud volcanoes also yielded consistent results [e.g., *Martin et al.*, 1996]. When applied to fluids from KC-27 and KC-14, geothermometers based on Na-K [*Fournier*, 1979] yield temperatures of 118°C and 138°C, respectively, and on Na-K-Ca [*Fournier and Truesdell*, 1973] yield temperatures of 136°C and 154°C, respectively. When applied to the Li-rich fluids sampled at the oil seep site, the Li-Na geothermometer of Kharaka and Mariner [*Kharaka and Mariner*, 1989] yields temperatures of 122°C and 132°C, almost identical to the Na-K geothermometer; however, the Li-Mg geothermometer [*Kharaka and Mariner*, 1989] results in 76°C–78°C for both cores. Silica geothermometers merely indicate near equilibrium with chalcedony at in situ temperature. The results for KC-27 are consistently 10°C–20°C lower than KC-14 suggesting a greater overprinting of low-temperature silicate diagenetic reactions at the former site. Overall the geothermometer analysis indicates that the fluid expelled at the hydrocarbon seeps reacted with the sediment within the 75°C–150°C temperature range. This maximum source temperature inferred for the fluids also corresponds to the upper limit of the seismogenic zone, assumed to occur 100°C–150°C [*Hyndman et al.*, 1997].

[29] In contrast to the other Marmara sites, the Western High mound fluids are brines of up to twice seawater concentration. The formation of hydrates surely drives this brine formation to some extent. For example, all components of the short core, KC-33, fall on a mixing line between pure water and a highly altered end-member nearly identical to the KC-14 end-member. Since this core had large amounts of gas hydrate, the composition is surely a result of water removal during hydrate formation and/or dissociation during core recovery. Cores KC-14 and KC-27 have nearly identical concentrations of K, Mg, and Li at their lowest depth, but differ by a factor of two in Ca and Sr concentration and by a factor of 1.3–1.4 in Cl and Na, precluding a sole gas hydrate cause for their concentrations. Halite dissolution from a buried

evaporite can also be ruled out as the brine source as the Na/Cl ratio would approach 1 rather than the observed trend lower to 0.6. A potential deep source for fluids at this site is the water associated with the reservoir from which the gas and oil is seeping. Oilfield waters are known to have strong enrichments of a variety of elements and often form brines [*Collins*, 1975]. Analysis of the gas and hydrate at the mound site suggests that the gas source is the same as that of the Kuzey Marmara gas field [*Bourry et al.*, 2009] which is located on a NE trending anticline that appears to be a continuation of the Sea of Marmara Western High. The source rock for this field is the Eocene Hamitabat Formation which consists of sandstone, shale, and conglomerate and the reservoir rock is the limestone Sogucak Formation [*Hosgormez and Yalcin*, 2005]. At the Kuzey Marmara field the Hamitabat formation is absent and the reservoir lies unconformably over the metamorphic basement which consists primarily of metamorphosed sedimentary rocks. Overlying formations consist primarily of shale, sandstone, siltstone, claystone, and conglomerates, and minor amounts of tuffite and is typically 1200–1500 m thick at the anticline crest [*Hosgormez and Yalcin*, 2005].

[30] While downcore increases in Ca and Sr and decreases in B, K, and Na are compatible with low-temperature silicate diagenetic processes, the unusually high Li concentrations are incompatible with a low-temperature diagenetic process. Li concentrations in the mound cores reach 1100 μM, a factor of nearly 40 greater than bottom water, while all other Marmara cores exhibit lower Li concentrations downcore. As a general rule, low-temperature diagenetic processes tend to take up Li while high-temperature processes release Li [*You and Gieskes*, 2001]. For example high Li is a common occurrence in fluids from oceanic high-temperature hydrothermal vents (300°C–400°C) in which seawater reacts with basaltic crust [e.g., *von Damm*, 1990]. High Li concentrations have also been observed in the deepest oil reservoirs of the Gulf of Mexico Basin [*Macpherson*, 1989]. Macpherson points out that such concentrations cannot be explained by mineral diagenesis or salt dissolution and must result from metamorphic processes occurring much deeper. High Li concentrations are also a common occurrence associated with the dehydration of smectite clays; however, these are nearly always also associated with low chlorinities and high B concentrations [e.g., *You et al.*, 1993] while, in our case, we have high chlorinities and lessening B concentrations downcore and an end-member B/Li molar ratio of 0.1–0.4. As pointed out by *Tryon et al.* [2010], B/Li molar ratios of less than 1 are extremely rare in marine sedimentary environments and are almost always associated with interaction with igneous rocks. In the continental environment, fluid-rock interactions with pegmatite veins in the metamorphic basement could also produce such fluid compositions; however, these are unknown in our Sea of Marmara study area.

[31] One possibility for a brine producing process that also produces fluids both high in Li and low in B is serpentinization. The serpentinization of ultramafic rocks takes up water and thus leaves a residual brine. Boron is also strongly taken up and Li leached from the rock during serpentinization [*Agranier et al.*, 2007; *Lee et al.*, 2008; *Snyder et al.*, 2005; *Vils et al.*, 2008]. This is indeed what is observed in deep boreholes in oceanic crust [*Expedition 309 and 312 Scientists*, 2006]. A potential source formation in the Marmara area is the IntraPontide suture zone. This accretionary complex is made up of serpentinized peridotites and igneous rocks, blueschist, radiolarian chert, and limestone [*Okay and Tüysüz*, 1999]. The Thrace Basin, presumably a fore-arc basin, was deposited over this complex and, in its northern part, on continental crust [*Görür and Okay*, 1996]. The western NAF roughly follows this suture zone; however, it is not known how this relationship continues beneath the Sea of Marmara. It is generally thought to intersect the Sea of Marmara in the east at the southern extension of the NAF, south of the Armutlu Peninsula, and in the west at the Ganos Fault [*Okay and Tüysüz*, 1999]. The suture may be offset from the southern NAF to the northern NAF (MMF) along the N–S trending West Black Sea Fault, a Cretaceous transform plate boundary, that intersects the Sea of Marmara in the north at the Central High. Thus, the MMF may cut this suture zone at depth at the Western High. We envision a deep hydrothermal system within the NAF and IntraPontide suture zone that feeds residual brines along fault zone conduits to overlying formations where it is further modified by mixing and diagenetic reactions to ultimately exit at the mounds.

[32] An intriguing additional related possibility exists for a source rock for the suggested serpentinization: an upper mantle sliver at depth in the transform fault, (e.g., as has also been suggested for the San Andreas Fault [*Ozacar and Zandt*, 2009]). Preliminary reports of He isotopic compositions of >1.0 Ra at Marmara fluid seeps [*Burnard and Bourlange*, 2008] also suggest that fluids origi-

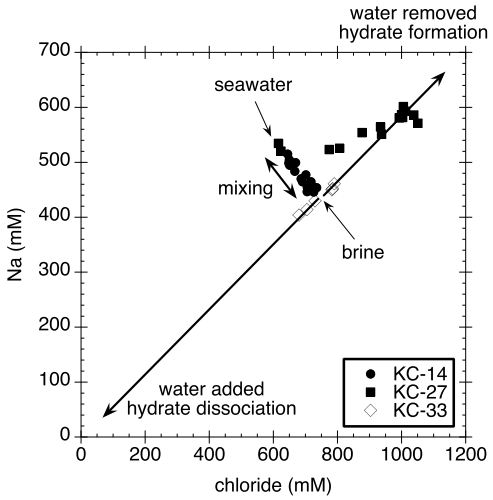

Figure 8. Plot of Cl versus Na for the mound site cores. KC-14 exhibits a simple mixing line between seawater and a brine end-member; KC-27 composition indicates a similar mixing of seawater and brine, overprinted by water removal during hydrate formation; and KC-33 falls on a mixing line between pure water and the brine indicating both removal of water by hydrate formation and addition of water during hydrate dissociation during core recovery and processing.

nating from subcrustal depths are expelled at the Marmara seafloor.

[33] Regardless of its source, a third fluid is, therefore, required to model the major ion composition of the fluids at the mound sites, KC-14, KC-27, and KC-33. There was no evidence of hydrate in core KC-14 and its end-member composition intersects the KC-33 hydrate water removal line, so this intersection is our best model for a brine end-member (Figure 8). Chloride is the only element that is assumed conservative in this analysis. There is no evidence for Lake Marmara brackish water at theses sites; however, its presence would be difficult to resolve in a hydrate environment given its similarity to pure water. The composition of the fluid sampled at the southern mound hydrate site (KC-27) would correspond approximately to the composition of the brine source if up to 25%–30% of the water flowing through is taken up by local hydrate formation. In this model, however, the initial K, Mg, and Li concentrations at the southern mound would be about 45% lower and Ca, Sr, and Ba about 25% higher than at the northern mound prior to hydrate formation. The proximity of the two sites virtually assures that they have a common deep source; therefore, differences in composition must be attributable to shallower, local effects such as low-temperature diagenetic reactions. Preliminary high-resolution 3-D seismic images from the 2009 Marmara-DM cruise suggest that the fluid conduits for the two mounds are separate to at least the depth of our resolution, about 250–300 m. Even at flow rates of up to 10 times that modeled from the KC-27 profile, fluid transit times in the conduits would be at least a thousand years, allowing time for significantly different fluid evolutions. These results, combined with the geothermometer results, suggest a much greater level of low-temperature silicate diagenesis at the southern mound.

[34] The sites exhibiting the clearest evidence for a deep aqueous fluid source are also sites of thermogenic gas expulsion [see *Bourry et al.*, 2009] and are located on anticlinal ridges, which can presumably act as fluid traps. Furthermore, the two carbonate and hydrate mounds are located some distance form the fault zone (350 and 700 m away along the ridge axis) and thus are probably outside of the damage zone of the main strike-slip fault. Our hypothesis to explain this is that the bulk of the fluids originate from the anticlinal traps rather than the fault zone itself. These traps probably extend several kilometers along the anticlines but may not be continuous. Where the anticline is breached by the fault, the interaction of MMF induced fractures and extensional fractures associated with the anticline allow fluids to escape. Much of the driving force of the fluid expulsion is gas and oil buoyancy and this will tend to exit at local highs, while the MMF on the Western High lies in a valley. Ultimately fluid outlet sites are controlled by a combination of local topography, fracture locations, and driving forces.

[35] In summary, the fluid samples collected during Marnaut suggest that part of the water expelled along the MMF at the ridges comes from at least thermogenic oil and gas generation depths. Anomalous He isotopic compositions [*Burnard and Bourlange*, 2008] and the low B/Li molar ratio brines are, so far, the main evidence that fluids originating from seismogenic or greater depths are expelled at the seafloor. Our samples also confirm that the fluids expelled along seafloor fault ruptures in the basins mostly originate at a shallow level in Pleistocene lacustrine sediments [*Zitter et al.*, 2008].

4.3. Factors Influencing the SMI

[36] Three cores taken at various locations away from fluid emission sites in the Çınarck and Central

Basin display nearly ideal linear sulfate profiles down to the SMI at 2.5 m depth, consistent with a simple diffusion-reaction model [e.g., *Halbach et al.*, 2004]. Sulfate concentration gradient is 11 mM/m in these cores. Considering that the tracer diffusion of sulfate in sediment is about half that of chloride [*Iversen and Jørgensen*, 1993] at about 1.5 m^2/yr for a sediment porosity of 70% and a temperature of 14°C, sulfate consumption, and hence methane flux, is estimated to 120 $mmol.m^{-2}.yr^{-1}$, in agreement with earlier estimates from the Sea of Marmara [*Çağatay et al.*, 2004],

[37] It is a remarkable paradox that, at several sites where the presence of free gas in the sediment is inferred from geophysical and/or visual observations (e.g., KC-17, VT-2737 and VT-2740 in Tekirdağ Basin, KC-19 and VT-2742 in the Central Basin, KC-26 on the western high), the SMI lies at a deeper level than in the reference cores. Overall, a relationship can be drawn between a sharp downward decrease of sulfate concentration above the SMI (gradient generally exceeds the 11 mM/m background value) and the depth at which chloride decreases below the 595 mM threshold. This relationship between sulfate concentration and chloride, a presumably conservative element, is puzzling. In fact, most of the chloride profiles near fluid emission sites are nearly constant to some depth within the sediment (typically 1 to 5 m) and start decreasing (or increasing in the case of cores KC-27 and KC-14) at the SMI or just above it. These profiles cannot be modeled with pore water advection-diffusion models unless some penetration of seawater in the sediment is considered. Various processes can, in principle, account for this observation: salinity driven convection [*Henry et al.*, 1992], bioirrigation [*Wallmann et al.*, 1997], episodic methane emission [*Tryon et al.*, 1999], eddy mixing in the wake of gas bubbles [*Haeckel et al.*, 2007]. All these processes require effective permeabilities in the upper few meters of sediment that would be considered atypical for clay rich sediments. However, one can hypothesize that wherever streams of small (1–5 mm diameter) bubbles are seen escaping through the seafloor, mm size conduits are present to some unknown depth in the sediment and influence water and chemical fluxes. As the primary objective of this manuscript is to identify fluid sources and diagenetic reactions, we save further discussion of fluxes through the seafloor for future work. We here merely point out that variations of the sulfate gradient with depth in the sediment may be caused by a steady state pore water irrigation process, rather than by migration of the SMI after an earthquake, as hypothesized by *Halbach et al.* [2004].

5. Summary and Conclusion

[38] Fluids expelled along the submerged western extension of the North Anatolian Fault Zone appear to be a mix of sources that have both separately and together undergone varying degrees of alteration by silicate and carbonate diagenetic processes and by gas hydrate formation. Major ion concentrations at most sites in the Sea of Marmara can be modeled from the mixing of up to three components: seawater, brackish water, and a hypothetical brine source extrapolated from core KC-14 pore fluid composition.

[39] The seeps in the southeastern Çınarck Basin are associated with distributed extension and expel fluids of primarily Pleistocene Lake Marmara and present-day seawater origin from relatively shallow depths. A small fraction of higher hydrocarbons suggests some contribution from a deeper source. Highly focused flow of Lake Marmara brackish water is observed both in the southeastern Tekirdağ Basin on the MMF and the eastern Central Basin at a fault branching point. All basin fluid compositions are overprinted to varying extent with local shallow redox reactions, carbonate precipitation, and barite dissolution. Basin consolidation and buoyancy drives low-density fluids into permeable turbidite layers and then laterally updip to basin bounding faults where they rise to be expelled at the surface. Site KC-19 at the NE edge of the central basin, KC-20 on the Central High, and, to a lesser extent KC-26 in the fault valley on the Western High are influenced by silicate diagenesis, but there is insufficient evidence to discriminate the contributions of shallower and deeper sources.

[40] At the Western High hydrate and carbonate mounds fluid composition is much more influenced by interaction with silicate minerals, suggesting a component of oil/gas reservoir or deeper brine is entrained with the oil and gas expulsion. The presence of oil and thermogenic gas, as well as results from geothermometers, suggests this fluid reacted with the rock in the 75°C–150°C temperature range. Low-temperature silicate diagenetic processes are also indicated, modifying the deep sourced fluids. In addition, formation and dissociation of gas hydrates near the seafloor (and dissociation during core recovery) drives compositional changes through water removal or addition One puzzling characteristics of the brine expelled at

this site is its very high lithium concentration and low B/Li ratio. This is atypical for fluids reacting with sediments during diagenesis, but could in theory be explained by interaction with mantle rocks. Such an explanation could be compatible with the geological context of the North Anatolian Fault in the Sea of Marmara. The nature of the interaction between the oil system and the fault is, however, a largely unsolved question. Hypothetically, the fracturing associated with strike-slip faulting may enhance fluid escape from oil reservoir and source rocks. Conversely, the crustal faults may provide fluids from even greater depths, and thus influence the composition of the reservoir fluids, and of the fluids expelled at the seafloor. More extensive exploration and coring along the anticline crests would help resolve this.

[41] While extensive research has been ongoing for nearly 20 years on fluid and gas seeps associated with subduction zone faults, submerged plate boundary transform faults present a new venue for such research. Our work here has shown that these environments can be hydrologically active and their fluid sources can be varied. The diversity of tectonic structures and fluid sources combined with a high level of tectonic activity with a long historical record makes the Sea of Marmara an exciting new locality for exploring the relationships between faulting, seismic activity and hydrogeology.

Acknowledgments

[42] We would like to thank Captain Michel Houmard and the crew of the R/V *L'Atalante* and Jean-Paul Justiniano, chief of the *Nautile* operation team, for their excellence in support of the science operations and the Turkish Navy for their support in protecting the ship and submersible in the zones of heavy ship traffic. We would also like to acknowledge Çelal Sengör and Naci Görür for their enthusiastic intellectual and logistical support of the Marnaut Project. Funding for this project was provided by NSF (OCE-0647361), INSU (Marmafluides Project), Ifremer, ANR (ISIS Project), and EC FP7 (ESONET Network of Excellence, MarmaraDM deliverable D1.3b). We also wish to thank Joris Gieskes, Ronan Apprioual, Gilbert Floch, Laurent Bignon, Jean-Claude Caprais, Marie-Agnes Angely, Muna Al-Samir, Ummuhan Sancar, Deniz Dikce, and Pat Rentz for their assistance.

References

Agranier, A., C.-T. A. Lee, X. A. Li, and W. P. Leeman (2007), Fluid mobile element budgets in serpentinized oceanic lithospheric mantle: Insights from B, As, Li, Pb, PGEs, and Os isotopes in the Feather River Ophiolite, California, *Chem. Geol.*, *245*, 230–241, doi:10.1016/j.chemgeo.2007.08.008.

Aksu, A., R. Hiscott, and D. Yasar (1999), Oscillating Quaternary water levels of the Marmara Sea and vigorous outflow into the Aegean Sea from the Marmara Sea–Black Sea drainage corridor, *Mar. Geol.*, *153*(1–4), 275–302, doi:10.1016/S0025-3227(98)00078-4.

Alpar, B. (1999), Underwater signatures of the Kocaeli Earthquake (August 17th 1999), *Turk. J. Mar. Sci.*, *5*, 111–130.

Armijo, R., B. Meyer, S. Navarro, and G. King (2002), Asymmetric slip partitioning in the Sea of Marmara pull-apart: A clue to propagation processes of the North Anatolian Fault?, *Terra Nova*, *14*, 80–86, doi:10.1046/j.1365-3121.2002.00397.x.

Armijo, R., et al. (2005), Submarine fault scarps in the Sea of Marmara pull-apart (North Anatolian Fault): Implications for seismic hazard in Istanbul, *Geochem. Geophys. Geosyst.*, *6*, Q06009, doi:10.1029/2004GC000896.

Barka, A., et al. (2002), The surface rupture and slip distribution of the 17 August 1999 Izmit earthquake (*M* 7.4), North Anatolian Fault, *Bull. Seismol. Soc. Am.*, *92*(1), 43–60, doi:10.1785/0120000841.

Bécel, A., M. Laigle, B. de Voogd, A. Hirn, T. Taymaz, S. Yolsal-Cevikbilen, and H. Shimamura (2010), North Marmara Trough architecture of basin infill, basement and faults, from PSDM reflection and OBS refraction seismics, *Tectonophysics*, *490*(1–2), 1–14, doi:10.1016/j.tecto.2010.04.004.

Borowski, W. S., C. K. Paull, and W. Ussler III (1996), Marine porewater sulfate profiles indicate in situ methane flux from underlying gas hydrate, *Geology*, *24*(7), 655–658, doi:10.1130/0091-7613(1996)024<0655:MPWSPI>2.3.CO;2.

Borowski, W. S., C. K. Paull, and W. Ussler III (1997), Carbon cycling within the upper methanogenic zone of continental rise sediments; An example from the methane-rich sediments overlying the Blake Ridge gas hydrate deposits, *Mar. Chem.*, *57*(3–4), 299–311, doi:10.1016/S0304-4203(97)00019-4.

Bourry, C., B. Chazallon, J. L. Charlou, J. P. Donval, L. Ruffine, P. Henry, L. Geli, M. N. Çağatay, S. İnan, and M. Moreau (2009), Free gas and gas hydrates from the Sea of Marmara, Turkey, *Chem. Geol.*, *264*(1–4), 197–206, doi:10.1016/j.chemgeo.2009.03.007.

Burnard, P., and S. Bourlange (2008), Helium isotope evidence for a deep source of fluids on the Marmara Fault, paper presented at ESONET NoE Training Course on Seafloor Observatory Techniques for Marine Geohazard Monitoring, Istanbul, Istanbul Tech. Univ., Istanbul, Turkey.

Çağatay, M. N., N. Gorur, O. Algan, C. Eastoe, A. Tchapalyga, D. Ongan, T. Kuhn, and I. Kuscu (2000), Late Glacial-Holocene paleooceanography of the Sea of Marmara: Timing of connections with the Mediterranean and the Black seas, *Mar. Geol.*, *167*, 191–206, doi:10.1016/S0025-3227(00)00031-1.

Çağatay, M., M. Ozcan, and E. Gungor (2004), Pore-water and sediment geochemistry in the Marmara Sea (Turkey): Early diagenesis and diffusive fluxes, *Geochem. Explor. Environ. Anal.*, *4*(3), 213–225, doi:10.1144/1467-7873/04-202.

Carton, H., et al. (2007), Seismic imaging of the three-dimensional architecture of the Çınarcık Basin along the North Anatolian Fault, *J. Geophys. Res.*, *112*, B06101, doi:10.1029/2006JB004548.

Collins, A. G. (1975), *Geochemistry of Oilfield Waters*, 496 pp., Elsevier, New York.

Demirbag, E., C. Rangin, X. L. Pichon, and A. M. C. Sengor (2003), Investigation of the tectonics of the Main Marmara Fault by means of deep towed seismic data, *Tectonophysics*, *361*(1–2), 1–19, doi:10.1016/S0040-1951(02)00535-8.

Dickens, G. R., M. Koelling, D. C. Smith, L. Schnieders, and the IODP Expedition 302 Scientists (2007), Rhizon sampling of pore waters on scientific drilling expeditions: An example from the IODP Expedition 302, Arctic Coring Expedition (ACEX), *Sci. Drill.*, *4*, 22–25.

Expedition 309 and 312 Scientists (2006), Superfast spreading rate crust 3: A complete in situ section of upper oceanic crust formed at a superfast spreading rate, *Prelim. Rep. Integrated Ocean Drill. Program*, *312*.

Flerit, F., R. Armijo, G. C. P. King, B. Meyer, and A. Barka (2003), Slip partitioning in the Sea of Marmara pull-apart determined from GPS velocity vectors, *Geophys. J. Int.*, *154*(1), 1–7, doi:10.1046/j.1365-246X.2003.01899.x.

Fournier, R. O. (1979), A revised equation for the Na/K geothermometer, *Trans. Geotherm. Res. Counc.*, *3*, 221–224.

Fournier, R. O., and A. H. Truesdell (1973), An empirical Na–K–Ca geothermometer for natural waters, *Geochim. Cosmochim. Acta*, *37*, 1255–1275, doi:10.1016/0016-7037(73)90060-4.

Géli, L., et al. (2008), Gas emissions and active tectonics within the submerged section of the North Anatolian Fault zone in the Sea of Marmara, *Earth Planet. Sci. Lett.*, *274*(1–2), 34–39, doi:10.1016/j.epsl.2008.06.047.

Gieskes, J. M., and J. R. Lawrence (1981), Alteration of volcanic matter in deep-sea sediments: Evidence from the chemical composition of interstitial waters from deep sea drilling cores, *Geochim. Cosmochim. Acta*, *45*, 1687–1703, doi:10.1016/0016-7037(81)90004-1.

Gieskes, J. M., T. Gamo, and H. Brumsack (1991), Chemical methods for interstitial water analysis aboard *JOIDES Resolution, Tech. Note 15*, 60 pp., Ocean Drill. Program, College Station, Tex.

Görür, N., and A. I. Okay (1996), A fore-arc origin for the Thrace Basin, NW Turkey, *Geol. Rundsch.*, *85*(4), 662–668, doi:10.1007/BF02440103.

Haeckel, M., B. P. Boudreau, and K. Wallmann (2007), Bubble-induced porewater mixing: A 3-D model for deep porewater irrigation, *Geochim. Cosmochim. Acta*, *71*, 5135–5154, doi:10.1016/j.gca.2007.08.011.

Halbach, P., and the Scientific Party (2000), Report and preliminary results of Meteor Cruise M44/1, in *Östliches Mittelmeer–Nördliches Rotes Meer 1999, Cruise No. 44, 22 January–16 May 1999. METEOR-Berichte*, edited by J. Pätzold et al., pp. 31–58, Univ. Hamburg, Hamburg, Germany.

Halbach, P., E. Holzbecher, T. Reichel, and R. Moche (2004), Migration of the sulphate–methane reaction zone in marine sediments of the Sea of Marmara—Can this mechanism be tectonically induced?, *Chem. Geol.*, *205*(1–2), 73–82, doi:10.1016/j.chemgeo.2003.12.013.

Henry, P., J.-P. Foucher, X. LePichon, M. Sibuet, K. Kobayashi, P. Tarits, N. Chamot-Rooke, T. Furuta, and P. J. Schultheiss (1992), Interpretation of temperature measurements from the Kaiko-Nankai cruise: Modeling of fluid flow in clam colonies, *Earth Planet. Sci. Lett.*, *109*, 355–371, doi:10.1016/0012-821X(92)90098-G.

Hergert, T., and O. Heidbach (2010), Slip-rate variability and distributed deformation in the Marmara Sea fault system, *Nat. Geosci.*, *3*, 132–135, doi:10.1038/ngeo739.

Hosgormez, H., and M. N. Yalcin (2005), Gas-source rock correlation in Thrace basin, Turkey, *Mar. Pet. Geol.*, *22*(8), 901–916, doi:10.1016/j.marpetgeo.2005.04.002.

Hovland, M., and H. Svensen (2006), Submarine pingoes: Indicators of shallow gas hydrates in a pockmark at Nyegga, Norwegian Sea, *Mar. Geol.*, *228*, 15–23, doi:10.1016/j.margeo.2005.12.005.

Hubert-Ferrari, A., A. Barka, E. Jacques, S. S. Nalbant, B. Meyer, R. Armijo, P. Tapponnier, and G. C. P. King (2000), Seismic hazard in the Marmara Sea region following the 17 August 1999 Izmit earthquake, *Nature*, *404*, 269–273, doi:10.1038/35005054.

Hyndman, R., M. Yamano, and D. A. Oleskevich (1997), The seismogenic zone of subduction thrust faults, *Isl. Arc*, *6*, 244–260, doi:10.1111/j.1440-1738.1997.tb00175.x.

Imren, C., X. L. Pichon, C. Rangin, E. Demirbag, B. Ecevitoglu, and N. Gorur (2001), The North Anatolian Fault within the Sea of Marmara: A new interpretation based on multi-channel seismic and multi-beam bathymetry data, *Earth Planet. Sci. Lett.*, *186*, 143–158, doi:10.1016/S0012-821X(01)00241-2.

Iversen, N., and B. B. Jørgensen (1993), Diffusion coefficients of sulfate and methane in marine sediments: Influence of porosity, *Geochim. Cosmochim. Acta*, *57*(3), 571–578, doi:10.1016/0016-7037(93)90368-7.

Judd, A., and M. Hovland (2007), *Seabed Fluid Flow: The Impact on Geology, Biology, and the Marine Environment*, doi:10.1017/CBO9780511535918, Cambridge Univ. Press, Cambridge, U. K.

Kazancı, N., Ö. Toprak, S. Leroy, S. Öncel, Ö. Ileri, Ö. Emre, P. Costa, K. Erturaç, and E. McGee (2006), Boron content of Lake Ulubat sediment: A key to interpret the morphological history of NW Anatolia, Turkey, *Appl. Geochem.*, *21*(1), 134–151, doi:10.1016/j.apgeochem.2005.09.003.

Kharaka, Y. K., and R. H. Mariner (1989), Chemical geothermometers and their application to formation waters from sedimentary basins, in *Thermal History of Sedimentary Basins*, edited by N. D. Naeser and T. H. McCulloh, pp. 99–117, Springer, New York.

Klaucke, I., D. Masson, C. J. Petersen, W. Weinrebe, and C. Ranero (2008), Multifrequency geoacoustic imaging of fluid escape structures offshore Costa Rica: Implications for the quantification of seep processes, *Geochem. Geophys. Geosyst.*, *9*, Q04010, doi:10.1029/2007GC001708.

Lee, C.-T. A., M. Oka, P. Luffi, and A. Agranier (2008), Internal distribution of Li and B in serpentinites from the Feather River Ophiolite, California, based on laser ablation inductively coupled plasma mass spectrometry, *Geochem. Geophys. Geosyst.*, *9*, Q12011, doi:10.1029/2008GC002078.

Le Pichon, X., et al. (2001), The active main Marmara fault, *Earth Planet. Sci. Lett.*, *192*, 595–616, doi:10.1016/S0012-821X(01)00449-6.

Le Pichon, X., N. Chamot-Rooke, C. Rangin, and A. M. C. Sengor (2003), The North Anatolian Fault in the Sea of Marmara, *J. Geophys. Res.*, *108*(B4), 2179, doi:10.1029/2002JB001862.

Levin, L. (2005), Ecology of cold seep sediments: Interactions of fauna with flow, chemistry and microbes, *Oceanogr. Mar. Biol. Annu. Rev.*, *43*, 1–46.

Luff, R., K. Wallmann, and G. Aloisi (2004), Numerical modeling of carbonate crust formation at cold vent sites: Significance for fluid and methane budgets and chemosynthetic biological communities, *Earth Planet. Sci. Lett.*, *221*(1–4), 337–353, doi:10.1016/S0012-821X(04)00107-4.

Macpherson, G. L. (1989), Lithium, boron, and barium in formation waters and sediments, northwestern Gulf of Mexico Sedimentary Basin, Ph.D. thesis, 305 pp., Univ. of Tex. at Austin, Austin.

Martin, J., M. Kastner, P. Henry, X. LePichon, and S. Lallement (1996), Chemical and isotopic evidence for sources of fluids in a mud volcano field seaward of the Barbados accretionary wedge, *J. Geophys. Res.*, *101*(B9), 20,325–20,345, doi:10.1029/96JB00140.

Meade, B. J., B. H. Hager, S. C. McClusky, R. Reilinger, S. Ergintav, O. Lenk, A. Barka, and H. Ozener (2002), Estimates of seismic potential in the Marmara Sea region from block models of secular deformation constrained by GPS measurements, *Bull. Seismol. Soc. Am.*, *92*, 208–215.

Mercier de Lépinay, B., L. Labeyrie, M. N. Çağatay, and the Marmacore Team (2003), Interplay between recent sedimentation and active tectonics in Marmara Sea, paper presented at European Geological Society–American Union of Geophysicists–European Union of Geophysicists General Assembly, Nice, France.

Okay, A. I., and O. Tüysüz (1999), Tehtyan sutures of northern Turkey, in *The Mediterranean Basin: Tertiary Extension Within the Alpine Orogen*, edited by B. Durand et al., pp. 475–515, Geol. Soc., London.

Ozacar, A. A., and G. Zandt (2009), Crustal structure and seismic anisotropy near the San Andreas Fault at Parkfield, California, *Geophys. J. Int.*, *178*, 1098–1104, doi:10.1111/j.1365-246X.2009.04198.x.

Parsons, T., S. Toda, R. S. Stein, A. Barka, and J. H. Dieterich (2000), Heightened odds of large earthquakes near Istanbul: An interaction-based probability calculation, *Science*, *288*, 661–665, doi:10.1126/science.288.5466.661.

Rangin, C., X. Le Pichon, E. Demirbag, and C. Imren (2004), Strain localization in the Sea of Marmara: Propagation of the North Anatolian Fault in a now inactive pull-apart, *Tectonics*, *23*, TC2014, doi:10.1029/2002TC001437.

Reilinger, R., et al. (2006), GPS constraints on continental deformation in the Africa-Arabia-Eurasia continental collision zone and implications for the dynamics of plate interactions, *J. Geophys. Res.*, *111*, B05411, doi:10.1029/2005JB004051.

Ryan, W. B. F., C. O. Major, G. Lericolais, and S. L. Goldstein (2003), Catastrophic flooding of the Black Sea, *Annu. Rev. Earth Planet. Sci.*, *31*(1), 525–554, doi:10.1146/annurev.earth.31.100901.141249.

Seeberg-Elverfeldt, J., M. Schluter, T. Feseker, and M. Kolling (2005), Rhizon sampling of porewaters near the sediment-water interface of aquatic systems, *Limnol. Oceanogr. Methods*, *3*, 361–371.

Snyder, G. T., I. P. Savov, and Y. Muramatsu (2005), Iodine and boron in Mariana serpentinite mud volcanoes (ODP Legs 125 and 195): Implications for forearc processes and subdution recycling [online], *Proc. Ocean Drill. Program Sci. Results*, *195*, 18 pp. (Available at http://www-odp.tamu.edu/publications/195_SR/102/102.htm)

Torres, M. E., J. McManus, D. Hammond, M. A. de Angelis, K. Heeschen, S. Colbert, M. D. Tryon, K. M. Brown, and E. Suess (2002), Fluid and chemical fluxes in and out of sediments hosting methane hydrate deposits on Hydrate Ridge, OR. I: Hydrological provinces, *Earth Planet. Sci. Lett.*, *201*(3–4), 525–540, doi:10.1016/S0012-821X(02)00733-1.

Tryon, M. D., and K. M. Brown (2004), Fluid and chemical cycling at Bush Hill: Implications for gas- and hydrate-rich environments, *Geochem. Geophys. Geosyst.*, *5*, Q12004, doi:10.1029/2004GC000778.

Tryon, M. D., K. M. Brown, M. E. Torres, A. M. Trehu, J. McManus, and R. W. Collier (1999), Measurements of transience and downward fluid flow near episodic methane gas vents, Hydrate Ridge, Cascadia, *Geology*, *27*(12), 1075–1078, doi:10.1130/0091-7613(1999)027<1075:MOTADF>2.3.CO;2.

Tryon, M., K. Brown, and M. Torres (2002), Fluid and chemical flux in and out of sediments hosting methane hydrate deposits on Hydrate Ridge, OR, II: Hydrological processes, *Earth Planet. Sci. Lett.*, *201*(3–4), 541–557, doi:10.1016/S0012-821X(02)00732-X.

Tryon, M. D., C. G. Wheat, and D. R. Hilton (2010), Fluid sources and pathways of the Costa Rica erosional convergent margin, *Geochem. Geophys. Geosyst.*, *11*, Q04S22, doi:10.1029/2009GC002818.

Verma, S. P., K. Pandarinath, and E. Santoyo (2008), SolGeo: A new computer program for solute geothermometers and its application to Mexican geothermal fields, *Geothermics*, *37*, 597–621, doi:10.1016/j.geothermics.2008.07.004.

Vidal, L., G. Menot, C. Joly, H. Bruneton, F. Rostek, M. N. Çağatay, C. Major, and E. Bard (2010), Hydrology in the Sea of Marmara during the last 23 ka: Implications for timing of Black Sea connections and sapropel deposition, Paleoceanography, 25, PA1205, doi:10.1029/2009PA001735.

Vils, F., L. Pelletier, A. Kalt, O. Müntener, and T. Ludwig (2008), The lithium, boron and beryllium content of serpentinized peridotites from ODP Leg 209 (Sites 1272A and 1274A): Implications for lithium and boron budgets of oceanic lithosphere, *Geochim. Cosmochim. Acta*, *72*(22), 5475–5504, doi:10.1016/j.gca.2008.08.005.

von Damm, K. (1990), Seafloor hydrothermal activity: Black smoker chemistry and chimneys, *Annu. Rev. Earth Planet. Sci.*, *18*(1), 173–204.

Wallmann, K., P. Linke, E. Suess, G. Bohrmann, H. Sahling, M. Schluter, A. Dahlmann, S. Lammers, J. Greinert, and N. von Mirbach (1997), Quantifying fluid flow, solute mixing, and biogeochemical turnover at cold vents of the eastern Aleutian subduction zone, *Geochim. Cosmochim. Acta*, *61*(24), 5209–5219, doi:10.1016/S0016-7037(97)00306-2.

You, C. F., and J. Gieskes (2001), Hydrothermal alteration of hemi-pelagic sediments: Experimental evaluation of geochemical processes in shallow subduction zones, *Appl. Geochem.*, *16*, 1055–1066, doi:10.1016/S0883-2927(01)00024-5.

You, C., A. Spivack, J. Smith, and J. Gieskes (1993), Mobilization of boron in convergent margins: Implications for the boron geochemical cycle, *Geology*, *21*(3), 207–210, doi:10.1130/0091-7613(1993)021<0207:MOBICM>2.3.CO;2.

Zitter, T. A. C., et al. (2008), Cold seeps along the main Marmara Fault in the Sea of Marmara (Turkey), *Deep Sea Res., Part I*, *55*, 552–570, doi:10.1016/j.dsr.2008.01.002.